Table 2. The number of small RNAs in serum detected by Illumina sequencing.

		Cutadapt		Mapping (miRBase)		Mapping (hg19)	
Sample	Total	No. of read	% read	No. of read	% read	No. of read	% read
PBC-1	9,996,912	5,912,672	59.14	582,682	9.85	5,195,131	87.86
PBC-2	17,103,184	8,147,153	47.64	837,575	10.28	6,484,515	79.59
PBC-3	11,731,105	9,001,730	76.73	873,985	9.71	5,414,933	60.15
PBC-4	12,785,162	10,700,147	83.69	1,463,341	13.68	8,227,422	76.89
PBC-5	14,732,479	9,138,080	62.03	1,125,157	12.31	7,317,178	80.07
PBC-6	12,139,379	7,256,738	59.78	1,274,462	17.56	5,612,279	77.34
PBC-7	12,895,734	10,107,477	78.38	1,067,578	10.56	7,826,537	77.43
PBC-8	18,786,941	11,711,844	62.34	967,802	8.26	8,323,607	71.07
PBC-9	11,852,431	8,980,873	75.77	1,141,912	12.71	7,593,581	84.55
PBC-10	18,224,562	12,752,337	69.97	756,930	5.94	8,912,212	69.89
CH-C-1	10,874,814	7,820,291	71.91	2,870,316	36.70	6,924,685	88.55
CH-C-2	10,242,500	8,138,815	79.46	3,250,159	39.93	6,976,754	85.72
CH-C-3	19,183,649	12,135,107	63.26	1,878,487	15.48	9,056,579	74.63
CH-C-4	18,750,568	15,952,136	85.08	1,877,654	11.77	14,829,719	92.96
CH-C-5	12,702,304	10,306,186	81.14	1,592,422	15.45	9,269,394	89.94
CH-B-1	5,861,013	4,732,185	80.74	1,126,751	23.81	3,708,378	78.37
CH-B-2	7,164,871	5,937,732	82.87	1,213,392	20.44	5,076,436	85.49
CH-B-3	7,029,349	6,357,274	90.44	858,562	13.51	5,378,310	84.60
CH-B-4	8,077,025	6,788,987	84.05	1,581,475	23.29	6,142,836	90.48
CH-B-5	10,255,895	9,101,104	88.74	1,952,400	21.45	7,687,217	84.46
Healthy-3	11,111,254	7,843,011	70.59	1,248,499	15.92	6,778,655	86.43
Healthy-4	12,449,813	10,690,833	85.87	2,410,128	22.54	9,204,163	86.09
Healthy-5	13,597,339	8,914,365	65.56	2,214,635	24.84	6,571,819	73.72
Healthy-7	11,351,494	9,825,442	86.56	1,880,266	19.14	8,618,696	87.72
Healthy-8	14,349,933	12,891,294	89.84	2,320,100	18.00	11,618,231	90.12
Total	313,249,710	231,143,813	73.79	38,366,670	16.60	188,749,267	81.66

doi:10.1371/journal.pone.0066086.t002

BIOCARTA showed that the genes of catenin (cadherin-associated protein), alpha 1 and similar to breast cancer anti-estrogen resistance 1 predicted target genes of the listed miRNAs, and played a role in cell-to-cell adhesion signaling pathway (Figure S1). The KEGG pathway indicated that the genes of baculoviral IAP repeat-containing 2, protein phosphatase 3 catalytic subunit beta isoform and tumor necrosis factor ligand superfamily member 10 were related to apoptosis (Figure S2).

Discussion

MiRNA changes in the liver have been reported in diseases such as HCC or chronic viral hepatitis. However, there is only limited information about their detection in blood and their correlations in PBC patients. The current study provides the first evidence that PBC is associated with altered miRNA expression. We have demonstrated that a number of miRNAs, especially hsa-miR-505-3p and miR-197-3p, were significantly differentially expressed in patients with PBC, leading to a unique miRNA expression profile in the diseased liver. Recently, many studies have examined several PBC associations with genes and there have been significant differences in the genetic risk loci reported [21] [30]. Therefore more carefully constructed studies will be needed to clarify, the pathogenesis of PBC, and the study of these differentially expressed miRNAs could serve in identifying biomarkers or lead to a better understanding of the underlying molecular mechanism that perpetuates PBC.

In our study, miRNA Illumina deep sequencing was first used to screen 10 PBC patients' sera. We were able to match the sample's sex because of particular importance for X-linked miRNA [31]. Then, qRT-PCR was used to confirm the result of deep sequencing.

Quantitative differential expression analysis identified a 81-miRNA signature distinguishing PBC, CH-C, CH-B and healthy controls. A hierarchical clustering analysis was performed utilizing the 81-miRNAs and their patterns separated the PBC from viral hepatitis and healthy controls. In addition, there were three subgroups (PBC-1,2,4,5, PBC-3,6,10 and PBC-7,8,9) in the PBC cluster. When comparing the subgroups, the PBC-3, 6,10 group showed an expression pattern that differed from those of the other two subgroups. As for the clinical background, PBC-6 patient that had been infected with hepatitis B virus were HBsAg negative and anti-HBc and anti-HBs positive, and PBC-10 patient had positive antinuclear antibodies (ANA) titers of 1:2560 or greater, while other patients had no serological evidence of HBV infection and no positive ANA titers of 1:160 or greater. However, there was no clear difference between the three subgroups in terms of the clinical stage. At present, there is no conclusive proof whether

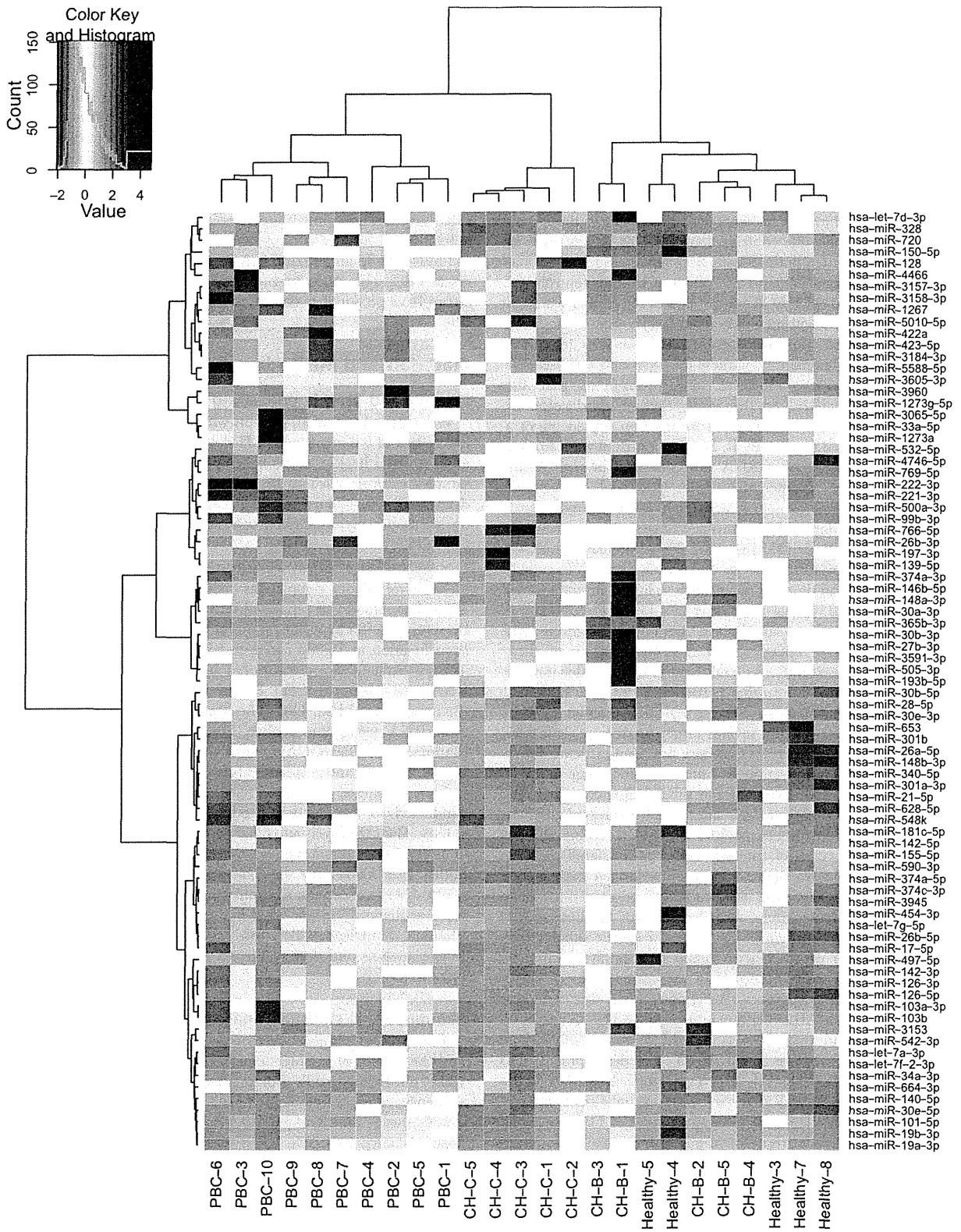

Figure 1. Heat map and hierarchical clustering. Individual miRNA expression were calculated by R platform and heat map was computed and described using a function of heatmap.2 in gplots. It uses hierarchical clustering with Euclidean distance; Pearson Linear Correlation and Ward's method to generate the hierarchical tree [56]. ANOVA was applied to extract differentially expressed miRNAs and adjustment of the p-value by

multiple comparisons was performed by calculating FDR. Those miRNAs with FDR<0.1 were presented. The red indicates high level of miRNA expression and the blue shows low.
doi:10.1371/journal.pone.0066086.g001

clinical or pathological differences can be found in clustering subgroups.

Nine miRNAs were confirmed to be significantly differentially expressed between the PBC group and viral hepatitis group or healthy control by Illumina deep sequencing. Among these 9 miRNAs, the serum levels of hsa-miR-505-3p and miR-197-3p were significantly lower in patients with PBC than in those with viral hepatitis and healthy controls, hsa-miR-139-5p was lower in patients with PBC than in those with viral hepatitis and miR-500a-3p were lower in patients with PBC than in healthy controls. Of note, we conducted qRT-PCR on the sera of some PBC who had already been treated with ursodeoxycholic acid. The serum levels of miRNA showed improvements in some samples (data not shown). Accordingly, quantifying these miRNAs may yield reliable diagnostic information. However, one problem is that the quantification of miRNA in this study used standardization by the total numbers of 1,000,000 reads in the deep sequencing or a comparative method in qRT-PCR. In other words, it was assumed that the same amount of miRNA was contained in each serum sample. Therefore, if one miRNA is quantified in a single specimen, we will not be able to accurately assess the result.

Specific circulating miRNA profiles have been reported for various diseases [32] [5] [33] [34] [35]. These circulating miRNA profiles have been described as correlating with differentially expressed miRNA in diseased tissue, such as liver injured by drugs or stomach afflicted with gastric cancer [36] [37]. Moreover, some disease-specific profiles can inform both the diagnosis and prognosis [38] [39]. Therefore, to determine if any of these diferentially expressed miRNAs could lead to better understanding of the molecular mechanism that perpetuates PBC, we examined for gene targets that may be reflected by this particular miRNA expression signature. Of the several target prediction algorithms prepared, we selected mirror 2.0. There has been evidence that a seed region of miRNA positioned within a limited range in the 3′ UTR of a target gene degrades the mRNA function [40]. We predicted 75 genes as targets for 9 differentially expressed miRNAs and conducted a functional analysis of DAVID. This analysis revealed that the genes of catenin (cadherin-associated protein), alpha 1 and similar to breast cancer anti-estrogen resistance 1 predicted target genes of the listed miRNA and played a role in cell-to-cell adhesion signaling, and the genes of baculoviral IAP repeat-containing 2, protein phosphatase 3 catalytic subunit beta isoform and tumor necrosis factor ligand superfamily member 10 were related to apoptosis. The onset of autoimmune disorders with PBC can be linked to apoptosis. A previous report described that the expression of TRAIL receptors is up-regulated by an increased bile acid level and that the serum level of soluble TRAIL is elevated, which may be involved in the development and progression of PBC [41,42]. However, further work will be required so that these miRNAs can serve not only as biomarkers but also for the elucidation of the pathogenesis of PBC.

GO analysis provides representations of biological annotations using precisely defined terms [43]. A previous report has described a number of genes involved in the signaling, regulation of I-kappaB kinase/NF-kappaB cascade and homeostasis that are associated with PBC [44] [45,46]. Additionally, our study indicated the biological processes, cellular component and molecular functions affected by the target genes included those associated with cell or membrane fraction, various kinds of ion binding and protein serine/threonine phosphatase complex, all of which are potentially related to PBC. Further studies will need to examine the relationship between differentially expressed miRNAs, both in serum and liver tissue, and target genes, which may provide more insights into the role of miRNAs in the pathology of PBC.

In conclusion, our results indicate that sera from patients with PBC have a unique miRNA expression profile compared to viral hepatitis and healthy controls and down-regulated expression of hsa-miR-505-3p and 197-3p may represent new clinical biomarkers in PBC. This study suggests that the amounts of miRNAs in serum have potential as diagnostic and prognostic biomarkers for PBC.

Materials and Methods

Patients and sample processing

We included sera of 10 patients with PBC who were treatment-naïve, sera of 5 patients with CH-B, sera of 5 patients with CH-C and sera of 5 healthy controls in this study. Initially these serum samples were enrolled to be analyzed by the Illumina miRNA deep sequencing (Illumina). The diagnosis of all cases was based on internationally established criteria [23].

Library preparation and Illumina sequencing

A ten ml venous sample was collected from each participant. The whole blood was separated into serum and cellular fractions by centrifugation at 2,500 r.p.m. for 10 min, followed by 10 min centrifugation at 10,000 r.p.m. to completely remove cell debris. The supernatant serum was stored at −20°C until analysis. Total RNA was extracted from 800 µl of serum using Trizol LS (Invitrogen, Carlsbad, CA). The libraries were constructed from total RNA using the TruSeq Small RNA Sample Prep Kit (Illumina, San Diego, CA) following the manufacturer's protocol. Briefly, RNA 3′ and 5′ adapters were ligated to target microRNAs in two separate steps. Reverse transcription reaction was conducted to the ligation products to create single stranded cDNA. The cDNA was amplified by PCR using a common primer and a primer containing the index sequence. One µl of each library was loaded on an Agilent Bioanalyzer (Agilent, Santa Clara, CA) to check the size, purity, and concentration. Libraries were sequenced on an Illumina GA IIx (SCS 2.8 software; Illumina, SanDiego, CA), with a 32-mer single end sequence. Image analysis and base calling were performed using RTA 1.8 software.

Sequence and statistical analysis

Raw miRNA sequence reads were conducted as a quality check and the 3′ and 5′ adapter sequences were removed by cutadapt while discarding reads shorter than 20 nucleotides [27]. The sequence reads were mapped with miRBase (Release 18) and UCSC (hg19) by use of bwa (0.5.9-r16), allowing one nucleotide base mismatch [47] [48].

Digital expression levels were normalized by taking into account the length of miRNAs and the total number of miRNA reads generated in each library using TMM normalization [28]. Read counts of each identified miRNA was normalized to the total number of miRNA reads, and then the ratio was multiplied by a constant set to 1×10^6 in this study. ANOVA was applied to extract differentially expressed miRNAs among the four groups. Adjustment of the p-value by multiple comparisons was performed by

Table 3. Differentially expressed miRNAs in serum from PBC patients compared with the second group (CH-C, CH-B, Healthy).

miRNA	Expression	PBC	CH-C	CH-B	Healthy	Fold change	p-value
		The mean no. of reads ±SE	The mean no. of reads ±SE	The mean no. of reads ±SE	The mean no. of reads ±SE		
hsa-miR-1273g-5p	Up	6.79±0.50	1.88±0.26	0.51±0.10	1.21±0.08	3.61	9.93E-03
hsa-miR-33a-5p	Up	6.19±1.59	0.10±0.04	1.58±0.23	2.20±0.18	2.82	4.07E-03
hsa-miR-3960	Up	11.26±0.59	4.85±0.51	3.63±0.27	1.86±0.24	2.32	4.27E-03
hsa-miR-766-5p	Down	0.17±0.04	2.92±0.53	1.55±0.10	0.64±0.12	0.27	4.61E-03
hsa-miR-505-3p	Down	5.05±0.22	16.23±0.89	26.81±3.99	16.73±1.54	0.31	3.40E-03
hsa-miR-30b-3p	Down	0.41±0.08	3.76±0.38	8.77±1.00	1.30±0.26	0.31	1.01E-03
hsa-miR-139-5p	Down	19.73±0.77	77.72±9.44	61.29±6.57	82.86±6.06	0.32	6.86E-03
hsa-miR-197-3p	Down	226.99±10.32	1067.05±106.41	589.88±60.38	823.16±66.17	0.38	7.76E-03
hsa-miR-500a-3p	Down	36.01±1.66	74.61±1.95	86.52±5.35	99.59±3.00	0.48	2.29E-03

doi:10.1371/journal.pone.0066086.t003

calculating FDR [49]. Those miRNAs with FDR<0.1 were extracted as differentially expressed and used in the following analysis. Hierarchical clustering was performed using an R platform and a heat map described as using a function of heatmap.2 in gplots [50].

qRT-PCR validation study

In addition to 25 samples analyzed by Illumina sequencing, five more serum samples of CH-B, CH-C and healthy controls (a total of 10 samples in each group) were used in qRT-PCR validation study. We followed the protocol previously reported by Mitchell *et al.* to determine the endogenous miRNA levels with spiked-in miRNA. Spiked-in miRNA was designed against *Caenorhabditis elegans* microRNA-39 (cel-miR-39) (5′- UCA CCG GGU GUA AAU CAG CUU -3′) and was synthesized by Sigma Aldrich Japan [32]. After total RNA isolation from 300 µl serum, reverse transcription was conducted using a TaqMan miRNA RT kit for identification of the cel-miR-39 expression (Applied Biosystems) with 5 fmol/µl for the internal control. qRT-PCR were conducted for detection of hsa-miR-1273g-5p, miR-505-3p and miR-139-5p in 20 µl PCR reactions using TaqMan MicroRNA assay with StepOne Plus detection system at 50°C for 2 min and 95°C for 10 min, followed by 40 cycles of 95°C for 15 s and 60°C for 1 min (Applied Biosystems). For detection of hsa-miR-33a-5p, miR-3960, miR-766-5p, miR-30b-3p, miR-197-3p and miR-500a-3p expression, we used the Exiqon system. Total RNA was reverse transcribed using the miRCURY LNA^{TM} Universal RT miRNA PCR, Polyadenylation and cDNA synthesis kit (Exiqon). cDNA diluted 50× was assayed in 10 µl PCR reactions according to the protocol for miRCURY LNA^{TM} Universal RT miRNA PCR with StepOne Plus detection system at 95°C for 10 min, followed by 40 cycles of 95°C for 10 s and 60°C for 1 min (Exiqon). The data were analyzed by the $2^{-\Delta\Delta Ct}$ method.

Statistical methods

Expression levels of the selected miRNAs detected by qRT-PCR were normalized to cel-miR-39 and presented as the fold-change ($2^{-\Delta\Delta Ct}$) above the control (CH-C-5): $\Delta\Delta Ct = (Ct_{miRNA}\text{-}Ct_{cel\text{-}miR\text{-}39})_{patients}\text{-}(Ct_{miRNA}\text{-}Ct_{cel\text{-}miR\text{-}39})_{CH\text{-}C\text{-}5}$. Results for normally distributed continuous variables are given as means (±standard errors of the mean) and compared between groups by Student's t-test. Results for non-normally distributed continuous variables are summarized as medians (interquartile ranges) and were compared by Mann-Whitney U test.

In silico analysis of miRNA target gene

For computational prediction of miRNA target genes, we used an algorithm: miRror 2.0 (June 2010 release, http://www.proto.cs.huji.ac.il/mirror/) [51]. MiRror 2.0 encompasses most of the available miRNA-target prediction tools covering human miRNAs. The algorithms used are collectively called miRNA-target prediction databases (MDBs): (i) PITA (Kartez); (ii) PicTar 4 (Krek); (iii) TargetRank (Nielsen); (iv) TargetScan (Lewis); (v) microCosm (John); (vi) miRanda (Betel); (vii) DIANA-microT (Maragkakis); (viii) MirZ (Hausser); (ix) miRDB (Wang); (x) RNA 22 (Miranda); (xi) MAMI (Sethupathy); (xii) miRNAMap2 (Hsu). The number of candidate genes and the number of miRNAs are indicated for each of the major MDBs. We selected as the search mode: miR2Gene; and as the search parameters of organism: human; and of selected tissue: all. Advanced parameters were inputted, cutoff: 0.01; database hits: 2; and target counts: 3. We created a list of common target genes for miRNAs. Then, these common targets were annotated by an annotation tool at the DAVID v6.7 (January 2010 release, http://david.abcc.ncifcrf.

Table 4. Clinical information of patients enrolled in the validation study.

	PBC (n = 10)	CH-C (n = 10)	CH-B (n = 10)	Healthy (n = 10)
Male/Female	2/8	4/6	6/4	6/4
Age range	51–72	47–70	27–72	26–62
Histological findings[a]				
Scheuer score	I (4) II (5) III (1)			
HAI		1 (1) 2 (8) 3 (1)	1 (3) 2 (4) 3 (3)	
T-bil (mg/dl)[b]	0.9 (0.5–1.2)	0.9 (0.6–1.5)	0.8 (0.5–1.1)	0.8 (0.6–1.0)
ALT (IU/l)[b]	42.4 (26–71)	47.1 (12–193)	139.1 (13–585)	25.8 (18–38)
ALP (IU/l)[b]	560.3 (404–800)	238.7 (167–403)	221.7 (111–319)	230.4 (148–302)
Albumin (g/dl)[b]	3.9 (3.4–4.2)	4.0 (3.5–4.2)	3.9 (3.7–4.4)	4 (3.8–4.3)
PT-INR[b]	0.97 (0.88–1.05)	1.02 (0.91–1.11)	1.07 (0.99–1.18)	1.07 (1.02–1.13)
AMA positivity	6			
M2 positivity	9			
HBV-DNA (Log copies/ml)[b]			6.2 (3.4–9.1)	
HCV-RNA (LogIU/ml)[b]		6.4 (5.1–7.3)		

[a]The numbers of patients are indicated in the parentheses.
[b]The range of laboratory data is indicated in the parentheses.
doi:10.1371/journal.pone.0066086.t004

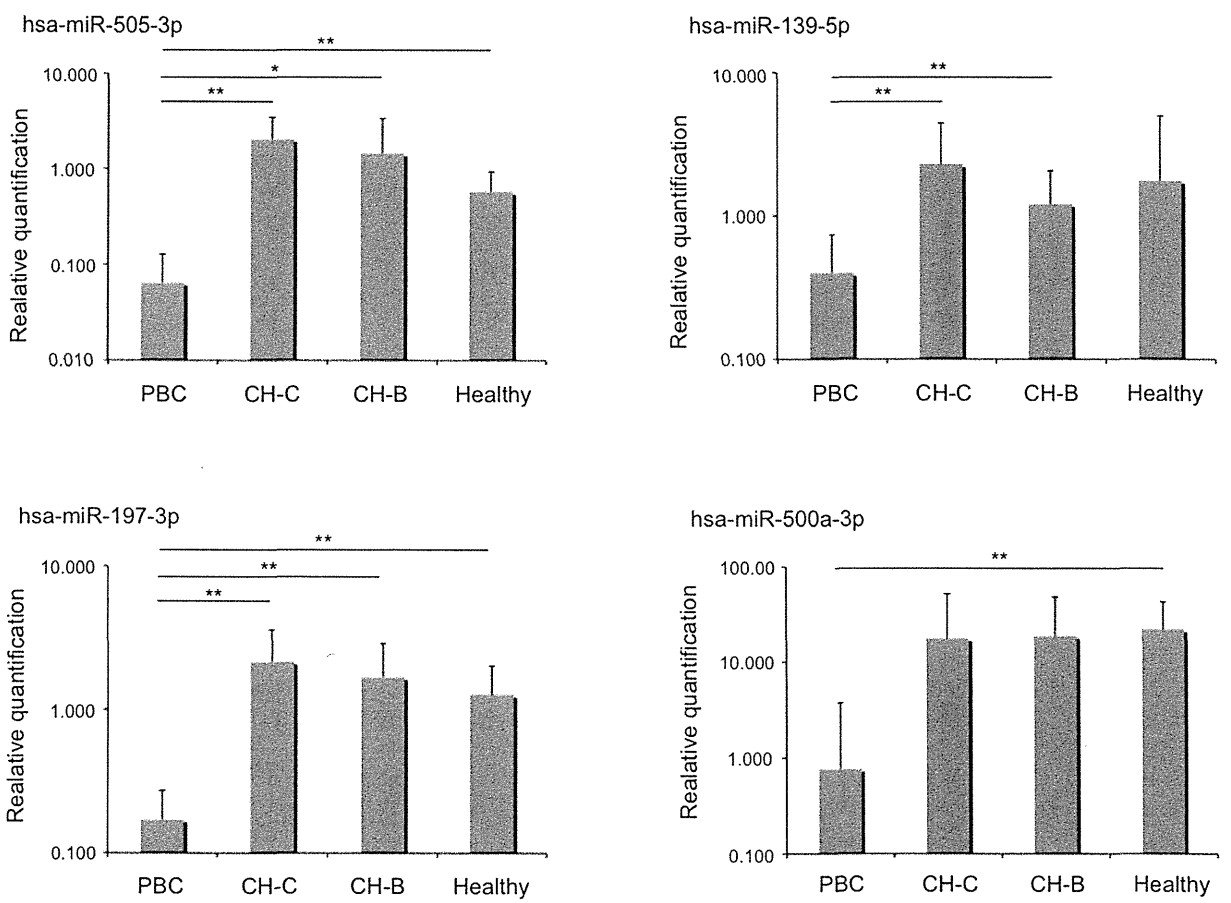

Figure 2. Validation of deep sequencing results for selected miRNAs. We have registered 10 samples in each group listed on Table S3. The threshold cycle for each miRNA primer/probe set were normalized with spiked in cel-miR-39 primer/probe pair and compared to CH-C-5. Result for normally distributed continuous variables are given as means and compared between groups by Student's t-test. Results for non-normally distributed continuous variables are summarized as medians and were compared by Mann-Whitney U test. Statistical significance indicates by one asterisk ($p<0.05$) and two ($p<0.01$).
doi:10.1371/journal.pone.0066086.g002

Table 5. Predicted target genes of 9 differentially expressed miRNA by Illumina sequencing in PBC.

Targets	Description	miRIS*	P-value
NM_000350	ATP-binding cassette, sub-family A (ABC1), member 4	0.250	1.83E-04
NM_000434	sialidase 1 (lysosomal sialidase) (NEU1), mRNA.	0.306	6.06E-04
NM_000491	complement component 1, q subcomponent, B chain	0.250	6.64E-04
NM_000663	4-aminobutyrate aminotransferase (ABAT), nuclear gene	0.417	9.55E-03
NM_000767	cytochrome P450, family 2, subfamily B, polypeptide 6	0.361	3.72E-03
NM_000878	interleukin 2 receptor, beta (IL2RB), mRNA.	0.250	7.10E-03
NM_001001716	nuclear factor of kappa light polypeptide gene	0.306	8.66E-03
NM_001007214	calcyclin binding protein (CACYBP), transcript variant	0.306	1.90E-03
NM_001012320	zinc finger protein 302 (ZNF302), transcript variant	0.306	3.32E-03
NM_001029997	zinc finger protein 181 (ZNF181), transcript variant	0.292	7.83E-03
NM_001033557	protein phosphatase 1B (formerly 2C),	0.250	7.51E-03
NM_001033910	TNF receptor-associated factor 5 (TRAF5), transcript	0.361	5.99E-03
NM_001034	ribonucleotide reductase M2 (RRM2), mRNA.	0.361	6.78E-03
NM_001098831	MORN repeat containing 4 (MORN4), transcript variant	0.306	4.68E-03
NM_001111125	IQ motif and Sec7 domain 2 (IQSEC2), transcript	0.361	2.49E-03
NM_001128932	cytochrome P450, family 4, subfamily F, polypeptide 11	0.361	8.47E-04
NM_001135146	solute carrier family 39 (zinc transporter), member 8	0.389	1.13E-03
NM_001136216	transmembrane protein 51 (TMEM51), transcript variant	0.250	2.75E-03
NM_001142289	mahogunin, ring finger 1 (MGRN1), transcript variant	0.361	7.27E-03
NM_001142353	protein phosphatase 3 (formerly 2B), catalytic	0.250	1.72E-03
NM_001142610	unc-51-like kinase 2 (C. elegans) (ULK2), transcript	0.347	5.97E-03
NM_001143944	LEM domain containing 2 (LEMD2), transcript variant 2,	0.250	2.08E-03
NM_001146699	RNA binding motif protein 19 (RBM19), transcript	0.306	6.81E-03
NM_001159322	phospholipase A2, group IVC (cytosolic,	0.292	1.32E-03
NM_001166	baculoviral IAP repeat-containing 2 (BIRC2), mRNA.	0.250	5.10E-03
NM_001293	chloride channel, nucleotide-sensitive, 1A (CLNS1A),	0.250	1.32E-03
NM_001337	chemokine (C-X3-C motif) receptor 1 (CX3CR1), mRNA.	0.417	1.39E-03
NM_001678	ATPase, Na+/K+ transporting, beta 2 polypeptide	0.417	4.07E-04
NM_001903	catenin (cadherin-associated protein), alpha 1, 102 kDa	0.389	3.97E-03
NM_002298	lymphocyte cytosolic protein 1 (L-plastin) (LCP1),	0.417	4.64E-03
NM_003810	tumor necrosis factor (ligand) superfamily, member 10	0.250	1.95E-03
NM_004414	regulator of calcineurin 1 (RCAN1), transcript variant	0.250	5.21E-03
NM_004642	cyclin-dependent kinase 2 associated protein 1	0.306	8.18E-04
NM_005046	kallikrein-related peptidase 7 (KLK7), transcript	0.306	7.63E-03
NM_005371	methyltransferase like 1 (METTL1), transcript variant	0.250	2.91E-03
NM_005517	high-mobility group nucleosomal binding domain 2	0.417	8.69E-03
NM_005736	ARP1 actin-related protein 1 homolog A, centractin	0.361	8.46E-03
NM_006598	solute carrier family 12 (potassium/chloride	0.361	5.04E-03
NM_014012	RAS (RAD and GEM)-like GTP-binding 1 (REM1), mRNA.	0.250	7.27E-03
NM_014452	tumor necrosis factor receptor superfamily, member 21	0.250	1.53E-03
NM_014567	breast cancer anti-estrogen resistance 1 (BCAR1),	0.250	6.32E-03
NM_014718	calsyntenin 3 (CLSTN3), mRNA.	0.250	3.78E-03
NM_014784	Rho guanine nucleotide exchange factor (GEF) 11	0.306	7.74E-03
NM_015278	SAM and SH3 domain containing 1 (SASH1), mRNA.	0.417	8.14E-03
NM_015352	protein O-fucosyltransferase 1 (POFUT1), transcript	0.472	1.47E-03
NM_016033	family with sequence similarity 82, member B (FAM82B),	0.458	3.43E-03
NM_016332	selenoprotein X, 1 (SEPX1), mRNA.	0.306	4.68E-03
NM_019072	small glutamine-rich tetratricopeptide repeat	0.417	8.71E-03
NM_019860	5-hydroxytryptamine (serotonin) receptor 7 (adenylate	0.250	7.39E-04

Table 5. Cont.

Targets	Description	miRIS*	P-value
NM_020211	RGM domain family, member A (RGMA), mRNA.	0.250	3.32E-03
NM_021131	protein phosphatase 2A activator, regulatory subunit 4	0.403	5.94E-03
NM_021939	FK506 binding protein 10, 65 kDa (FKBP10), mRNA.	0.306	1.13E-03
NM_021943	zinc finger, AN1-type domain 3 (ZFAND3), mRNA.	0.306	1.60E-03
NM_022497	mitochondrial ribosomal protein S25 (MRPS25), nuclear	0.417	8.60E-03
NM_024025	dual specificity phosphatase 26 (putative) (DUSP26),	0.403	1.66E-03
NM_024596	microcephalin 1 (MCPH1), mRNA.	0.361	1.00E-03
NM_024637	galactose-3-O-sulfotransferase 4 (GAL3ST4), mRNA.	0.361	1.73E-03
NM_024667	vacuolar protein sorting 37 homolog B (S. cerevisiae)	0.306	3.92E-03
NM_024898	DENN/MADD domain containing 1C (DENND1C), mRNA.	0.250	7.54E-03
NM_025108	chromosome 16 open reading frame 59 (C16orf59), mRNA.	0.250	3.39E-03
NM_031287	splicing factor 3b, subunit 5, 10kDa (SF3B5), mRNA.	0.306	4.48E-03
NM_032139	ankyrin repeat domain 27 (VPS9 domain) (ANKRD27),	0.306	9.38E-03
NM_032497	zinc finger protein 559 (ZNF559), mRNA.	0.347	4.45E-03
NM_080678	ubiquitin-conjugating enzyme E2F (putative) (UBE2F),	0.347	3.60E-03
NM_138396	membrane-associated ring finger (C3HC4) 9 (MARCH9),	0.306	5.18E-04
NM_138799	membrane bound O-acyltransferase domain containing 2	0.361	7.92E-03
NM_145168	short chain dehydrogenase/reductase family 42E, member	0.306	8.59E-03
NM_147202	chromosome 9 open reading frame 25 (C9orf25), mRNA.	0.417	4.67E-03
NM_173509	family with sequence similarity 163, member A	0.361	2.90E-03
NM_175839	spermine oxidase (SMOX), transcript variant 1, mRNA.	0.361	4.28E-03
NM_178468	family with sequence similarity 83, member C (FAM83C),	0.250	4.68E-03
NM_178832	MORN repeat containing 4 (MORN4), transcript variant	0.306	4.68E-03
NM_178835	zinc finger protein 827 (ZNF827), mRNA.	0.361	5.67E-03
NM_182527	calcium binding protein 7 (CABP7), mRNA.	0.417	1.95E-03
NM_198853	tripartite motif-containing 74 (TRIM74), mRNA.	0.403	1.82E-03

*miRIS :miRror Internal Score ranges from 0 top 1 by average 2 components (number of databases and input hits).
doi:10.1371/journal.pone.0066086.t005

gov/) [52]. DAVID can detect functional enrichment of a gene list based on the GO terms, KEGG pathway and BIOCARTA pathway. Differences were considered significant when the P value was less than 0.05.

Ethics statement

This study was approved by the Ethics Committee of the Tohoku University School of Medicine (2010-404) and written informed consent was obtained from each individual.

Supporting Information

Figure S1 The pathway of cell-to-cell adhesion signaling. The functional annotation analysis of BIOCARTA showed that the genes of catenin (cadherion-associated protein), alpha 1 and similar to breast cancer anti-estrogen resistance 1 played roles in this pathway. The stars indicate the related genes.
(TIFF)

Figure S2 The pathway of apoptosis. The functional annotation analysis of BIOCARTA showed that the genes of baculoviral IAP repeat-containing 2, protein phosphatase 3 (formerly 2B), catalytic subunit, beta isoform and tumor necrosis factor (ligand) superfamily, member 10 was related to apoptosis. The gene is indicated with the stars.
(TIFF)

Table S1 The list of differential expression levels of miRNA in each sample.
(XLS)

Table S2 Biological function analysis in GO terms of predicted gene targets of differentially regulated miRNAs using DAVID.
(DOC)

Acknowledgments

We thank M. Tsuda, M. Kikuchi, N. Koshita and K. Kuroda for technical assistance. We also acknowledge the support of the Biomedical Research Core of Tohoku University Graduate School of Medicine.

Accession number of DNA data bank of Japan (DDBJ) for the deep-sequence data reported in this paper is DRA000933.

Author Contributions

Conceived and designed the experiments: TS KN YU YK MN. Performed the experiments: MN RF. Analyzed the data: MN TN. Contributed reagents/materials/analysis tools: YK TK EK OK. Wrote the paper: MN YU.

References

1. Lau NC, Lim LP, Weinstein EG, Bartel DP (2001) An abundant class of tiny RNAs with probable regulatory roles in Caenorhabditis elegans. Science 294: 858–862.
2. Lagos-Quintana M, Rauhut R, Lendeckel W, Tuschl T (2001) Identification of novel genes coding for small expressed RNAs. Science 294: 853–858.
3. Lee RC, Ambros V (2001) An extensive class of small RNAs in Caenorhabditis elegans. Science 294: 862–864.
4. Bartel DP (2004) MicroRNAs: genomics, biogenesis, mechanism, and function. Cell 116: 281–297.
5. Chen X, Ba Y, Ma L, Cai X, Yin Y, et al. (2008) Characterization of microRNAs in serum: a novel class of biomarkers for diagnosis of cancer and other diseases. Cell Research 18: 997–1006.
6. Lu J, Getz G, Miska EA, Alvarez-Saavedra E, Lamb J, et al. (2005) MicroRNA expression profiles classify human cancers. Nature 435: 834–838.
7. Bihrer V, Friedrich-Rust M, Kronenberger B, Forestier N, Haupenthal J, et al. (2011) Serum miR-122 as a biomarker of necroinflammation in patients with chronic hepatitis C virus infection. Am J Gastroenterol 106: 1663–1669.
8. Zhang Y, Jia Y, Zheng R, Guo Y, Wang Y, et al. (2010) Plasma microRNA-122 as a biomarker for viral-, alcohol-, and chemical-related hepatic diseases. Clin Chem 56: 1830–1838.
9. Cermelli S, Ruggieri A, Marrero JA, Ioannou GN, Beretta L (2011) Circulating MicroRNAs in Patients with Chronic Hepatitis C and Non-Alcoholic Fatty Liver Disease. PLoS One 6: e23937.
10. Morita K, Taketomi A, Shirabe K, Umeda K, Kayashima H, et al. (2011) Clinical significance and potential of hepatic microRNA-122 expression in hepatitis C. Liver Int 31: 474–484.
11. Li LM, Hu ZB, Zhou ZX, Chen X, Liu FY, et al. (2010) Serum microRNA Profiles Serve as Novel Biomarkers for HBV Infection and Diagnosis of HBV-Positive Hepatocarcinoma. Cancer Research 70: 9798–9807.
12. Nakanuma Y, Ohta G (1979) Histometric and serial section observations of the intrahepatic bile ducts in primary biliary cirrhosis. Gastroenterology 76: 1326–1332.
13. Gershwin ME, Mackay IR, Sturgess A, Coppel RL (1987) Identification and specificity of a cDNA encoding the 70 kd mitochondrial antigen recognized in primary biliary cirrhosis. J Immunol 138: 3525–3531.
14. Coppel RL, McNeilage LJ, Surh CD, Van de Water J, Spithill TW, et al. (1988) Primary structure of the human M2 mitochondrial autoantigen of primary biliary cirrhosis: dihydrolipoamide acetyltransferase. Proc Natl Acad Sci U S A 85: 7317–7321.
15. Selmi C, Mayo MJ, Bach N, Ishibashi H, Invernizzi P, et al. (2004) Primary biliary cirrhosis in monozygotic and dizygotic twins: genetics, epigenetics, and environment. Gastroenterology 127: 485–492.
16. Begovich AB, Klitz W, Moonsamy PV, Van de Water J, Peltz G, et al. (1994) Genes within the HLA class II region confer both predisposition and resistance to primary biliary cirrhosis. Tissue Antigens 43: 71–77.
17. Donaldson PT, Baragiotta A, Heneghan MA, Floreani A, Venturi C, et al. (2006) HLA class II alleles, genotypes, haplotypes, and amino acids in primary biliary cirrhosis: a large-scale study. Hepatology 44: 667–674.
18. Onishi S, Sakamaki T, Maeda T, Iwamura S, Tomita A, et al. (1994) DNA typing of HLA class II genes; DRB1*0803 increases the susceptibility of Japanese to primary biliary cirrhosis. J Hepatol 21: 1053–1060.
19. Hirschfield GM, Liu X, Xu C, Lu Y, Xie G, et al. (2009) Primary biliary cirrhosis associated with HLA, IL12A, and IL12RB2 variants. N Engl J Med 360: 2544–2555.
20. Mells GF, Floyd JA, Morley KI, Cordell HJ, Franklin CS, et al. (2011) Genome-wide association study identifies 12 new susceptibility loci for primary biliary cirrhosis. Nat Genet 43: 329–332.
21. Hirschfield G, Invernizzi P (2011) Progress in the Genetics of Primary Biliary Cirrhosis. Seminars in Liver Disease 31: 147–156.
22. Nakamura M, Nishida N, Kawashima M, Aiba Y, Tanaka A, et al. (2012) Genome-wide Association Study Identifies TNFSF15 and POU2AF1 as Susceptibility Loci for Primary Biliary Cirrhosis in the Japanese Population. Am J Hum Genet 91: 721–728.
23. Lindor KD, Gershwin ME, Poupon R, Kaplan M, Bergasa NV, et al. (2009) Primary biliary cirrhosis. Hepatology 50: 291–308.
24. Corpechot C, Poupon R (2007) Geotherapeutics of primary biliary cirrhosis: Bright and sunny around the Mediterranean but still cloudy and foggy in the United Kingdom. Hepatology 46: 963–965.
25. Metcalf JV, Mitchison HC, Palmer JM, Jones DE, Bassendine MF, et al. (1996) Natural history of early primary biliary cirrhosis. Lancet 348: 1399–1402.
26. Gilad S, Meiri E, Yogev Y, Benjamin S, Lebanony D, et al. (2008) Serum microRNAs are promising novel biomarkers. PLoS One 3: e3148.
27. Martin M (2011) Cutadapt removes adapter sequences from high-throughput sequencing reads. EMBnet journal 17: 10–12.
28. Robinson MD, Oshlack A (2010) A scaling normalization method for differential expression analysis of RNA-seq data. Genome Biology 11: R25.
29. Balaga O, Friedman Y, Linial M (2012) Toward a combinatorial nature of microRNA regulation in human cells. Nucleic Acids Res 40: 9404–9416.
30. Juran BD, Lazaridis KN (2010) Update on the genetics and genomics of PBC. J Autoimmun 35: 181–187.
31. Zhang R, Peng Y, Wang W, Su B (2007) Rapid evolution of an X-linked microRNA cluster in primates. Genome Res 17: 612–617.
32. Mitchell PS, Parkin RK, Kroh EM, Fritz BR, Wyman SK, et al. (2008) Circulating microRNAs as stable blood-based markers for cancer detection. Proceedings of the National Academy of Sciences 105: 10513–10518.
33. Ai J, Zhang R, Li Y, Pu J, Lu Y, et al. (2010) Circulating microRNA-1 as a potential novel biomarker for acute myocardial infarction. Biochemical and Biophysical Research Communications 391: 73–77.
34. Chim SSC, Shing TKF, Hung ECW, Leung Ty, Lau Tk, et al. (2008) Detection and Characterization of Placental MicroRNAs in Maternal Plasma. Clinical Chemistry 54: 482–490.
35. Starkey Lewis PJ, Dear J, Platt V, Simpson KJ, Craig DGN, et al. (2011) Circulating microRNAs as potential markers of human drug-induced liver injury. Hepatology 54: 1767–1776.
36. Wang K, Zhang S, Marzolf B, Troisch P, Brightman A, et al. (2009) Circulating microRNAs, potential biomarkers for drug-induced liver injury. Proceedings of the National Academy of Sciences 106: 4402–4407.
37. Tsujiura M, Ichikawa D, Komatsu S, Shiozaki A, Takeshita H, et al. (2010) Circulating microRNAs in plasma of patients with gastric cancers. British Journal of Cancer 102: 1174–1179.
38. Kong X, Du Y, Wang G, Gao J, Gong Y, et al. (2010) Detection of Differentially Expressed microRNAs in Serum of Pancreatic Ductal Adenocarcinoma Patients: miR-196a Could Be a Potential Marker for Poor Prognosis. Digestive Diseases and Sciences 56: 602–609.
39. Silva J, Garcia V, Zaballos A, Provencio M, Lombardia L, et al. (2010) Vesicle-related microRNAs in plasma of nonsmall cell lung cancer patients and correlation with survival. European Respiratory Journal 37: 617–623.
40. Li M, Marin-Muller C, Bharadwaj U, Chow K-H, Yao Q, et al. (2008) MicroRNAs: Control and Loss of Control in Human Physiology and Disease. World Journal of Surgery 33: 667–684.
41. Berg CP, Stein GM, Keppeler H, Gregor M, Wesselborg S, et al. (2007) Apoptosis-associated antigens recognized by autoantibodies in patients with the autoimmune liver disease primary biliary cirrhosis. Apoptosis 13: 63–75.
42. Liang Y, Yang Z, Li C, Zhu Y, Zhang L, et al. (2008) Characterisation of TNF-related apoptosis-inducing ligand in peripheral blood in patients with primary biliary cirrhosis. Clinical and Experimental Medicine 8: 1–7.
43. Ashburner M, Ball CA, Blake JA, Botstein D, Butler H, et al. (2000) Gene ontology: tool for the unification of biology. The Gene Ontology Consortium. Nat Genet 25: 25–29.
44. Nakagome Y, Ueno Y, Kogure T, Fukushima K, Moritoki Y, et al. (2007) Autoimmune cholangitis in NOD.c3c4 mice is associated with cholangiocyte-specific Fas antigen deficiency. J Autoimmun 29: 20–29.
45. Singh R, Bullard J, Kalra M, Assefa S, Kaul AK, et al. (2011) Status of bacterial colonization, Toll-like receptor expression and nuclear factor-kappa B activation in normal and diseased human livers. Clinical Immunology 138: 41–49.
46. Kyriakou DS, Alexandrakis MG, Zachou K, Passam F, Stathakis NE, et al. (2003) Hemopoietic progenitor cells and bone marrow stromal cells in patients with autoimmune hepatitis type 1 and primary biliary cirrhosis. J Hepatol 39: 679–685.
47. Maglott D, Ostell J, Pruitt KD, Tatusova T (2010) Entrez Gene: gene-centered information at NCBI. Nucleic Acids Research 39: D52–D57.
48. Kozomara A, Griffiths-Jones S (2010) miRBase: integrating microRNA annotation and deep-sequencing data. Nucleic Acids Research 39: D152–D157.
49. Benjamini Y, Hochberg Y (1995) Controlling the false discovery rate: A practical and powerful approach to multiple testing. Journal of the Royal Statistical Society 57: 289–300.
50. Team RDC (2011) R: a language and environment for statistical computing. Vienna, Austria: the R Foundation for Statistical Computing.
51. Friedman Y, Naamati G, Linial M (2010) MiRror: a combinatorial analysis web tool for ensembles of microRNAs and their targets. Bioinformatics 26: 1920–1921.
52. Dennis G, Jr., Sherman BT, Hosack DA, Yang J, Gao W, et al. (2003) DAVID: Database for Annotation, Visualization, and Integrated Discovery. Genome Biol 4: P3.
53. Knodell RG, Ishak KG, Black WC, Chen TS, Craig R, et al. (1981) Formulation and application of a numerical scoring system for assessing histological activity in asymptomatic chronic active hepatitis. Hepatology 1: 431–435.
54. Ludwig J, Dickson ER, McDonald GS (1978) Staging of chronic nonsuppurative destructive cholangitis (syndrome of primary biliary cirrhosis). Virchows Arch A Pathol Anat Histol 379: 103–112.
55. Scheuer P (1967) Primary biliary cirrhosis. Proceedings of the Royal Society of Medicine 60: 1257–1260.
56. Ward JH (1963) Hierarchical Grouping to Optimize an Objective Function. Journal of the American Statistical Association 58: 236–244.

HEPATOLOGY
Official Journal of the American Association for the Study of Liver Diseases

AUTOIMMUNE, CHOLESTATIC AND BILIARY DISEASE

GABA Induces the Differentiation of Small Into Large Cholangiocytes by Activation of Ca^{2+}/CaMK I-Dependent Adenylyl Cyclase 8

Romina Mancinelli,[5] Antonio Franchitto,[5,6] Shannon Glaser,[1,2,3] Fanyin Meng,[1,2,3,4] Paolo Onori,[7] Sharon DeMorrow,[2,3] Heather Francis,[1,2,3,4] Julie Venter,[3] Guido Carpino,[8] Kimberley Baker,[1,2] Yuyan Han,[3] Yoshiyuki Ueno,[9,10] Eugenio Gaudio,[5*] and Gianfranco Alpini[1,2,3*]

Large, but not small, cholangiocytes (1) secrete bicarbonate by interaction with secretin receptors (SRs) through activation of cystic fibrosis transmembrane regulator (CFTR), Cl^-/HCO_3^- (apex) anion exchanger 2 (Cl^-/HCO_3^- AE2), and adenylyl cyclase (AC)8 (proteins regulating large biliary functions) and (2) proliferate in response to bile duct ligation (BDL) by activation of cyclic adenosine monophosphate (cAMP) signaling. Small, mitotically dormant cholangiocytes are activated during damage of large cholangiocytes by activation of D-*myo*-inositol 1,4,5-trisphosphate/Ca^{2+}/calmodulin-dependent protein kinase (CaMK) I. gamma-Aminobutyric acid (GABA) affects cell functions by modulation of Ca^{2+}-dependent signaling and AC. We hypothesized that GABA induces the differentiation of small into large cholangiocytes by the activation of Ca^{2+}/CaMK I-dependent AC8. *In vivo*, BDL mice were treated with GABA in the absence or presence of 1,2-bis-(o-aminophenoxy)-ethane-N,N,N′,N′-tetraacetic acid, tetraacetoxymethyl ester (BAPTA/AM) or N-(6-aminohexyl)-5-chloro-1-naphtalenesulfonamide (W7) before evaluating apoptosis and intrahepatic bile ductal mass (IBDM) of small and large cholangiocytes. *In vitro*, control- or CaMK I-silenced small cholangiocytes were treated with GABA for 3 days before evaluating apoptosis, proliferation, ultrastructural features, and the expression of CFTR, Cl^-/HCO_3^- AE2, AC8, and secretin-stimulated cAMP levels. *In vivo* administration of GABA induces the apoptosis of large, but not small, cholangiocytes and decreases large IBDM, but increased *de novo* small IBDM. GABA stimulation of small IBDM was blocked by BAPTA/AM and W7. Subsequent to GABA *in vitro* treatment, small cholangiocytes *de novo* proliferate and acquire ultrastructural and functional phenotypes of large cholangiocytes and respond to secretin. GABA-induced changes were prevented by BAPTA/AM, W7, and stable knockdown of the CaMK I gene. *Conclusion*: GABA damages large, but not small, cholangiocytes that differentiate into large cholangiocytes. The differentiation of small into large cholangiocytes may be important in the replenishment of the biliary epithelium during damage of large, senescent cholangiocytes. (HEPATOLOGY 2013;58:251-263)

The intrahepatic biliary epithelium is a network of interconnecting ducts of different functions and sizes,[1,2] with small ducts (<15 μm in diameter) lined by small cholangiocytes (~8 μm in size) and larger ducts (>15 μm in diameter) lined by larger cholangiocytes (~15 μm in size).[1,3]

Abbreviations: Abs, antibodies; AC, adenylyl cyclase; BAPTA/AM, 1,2-bis-(o-aminophenoxy)-ethane-N,N,N′,N′-tetraacetic acid, tetraacetoxymethyl ester; BDL, bile duct ligation; b.w., body weight; BSA, bovine serum albumin; cAMP, cyclic adenosine monophosphate; CaMK, calmodulin-dependent protein kinase; CFTR, cystic fibrosis transmembrane regulator; Cl^-/HCO_3^- AE2, Cl^-/HCO_3^- anion exchanger 2; GABA, gamma-aminobutyric acid; GAPDH, glyceraldehyde-3-phosphate dehydrogenase; H&E, hematoxylin and eosin; IBDM, intrahepatic bile duct mass; IF, immunofluorescence; IHC, immunohistochemistry; IP, intraperitoneal; IP_3, D-myo-inositol 1,4,5-trisphosphate; GABA, gamma-aminobutyric acid; mRNA, messenger RNA; PCNA, proliferating cellular nuclear antigen; PCR, polymerase chain reaction; PKC, protein kinase C; RIA, radioimmunoassay; SEM, standard error of the mean; shRNA, short hairpin RNA; SR, secretin receptor; TUNEL, quantitative terminal deoxynucleotidyl transferase biotin-dUTP nick-end labeling; W7, N-(6-aminohexyl)-5-chloro-1-naphtalenesulfonamide.

From the [1]Department of Research, Central Texas Veterans Health Care System, [2]Scott & White Digestive Disease Research Center, [3]Division of Gastroenterology, Department of Medicine College of Medicine, and [4]Division of Research and Education, Scott & White Digestive Diseases Research Center, Texas A&M Health Science Center, Temple, TX; [5]Department of Anatomical, Histological, Forensic Medicine and Orthopedics Sciences, University "Sapienza", Rome, Italy; [6]Eleonora Lorillard Spencer Cenci Foundation, Rome, Italy; [7]Experimental Medicine, University of L'Aquila, L'Aquila, Italy; [8]Department of Health Science, IUSM University of Rome, Italy; [9]Department Gastroenterology, Yamagata University Faculty of Medicine, Yamagata, Japan; and [10]CREST, Yamagata, Japan.

Received November 21, 2012; accepted January 31, 2013.

Cholangiocytes regulate the homeostasis of the biliary epithelium by affecting the functions of this system by activation of Ca^{2+}- (small cholangiocytes)[4] and/or cyclic adenosine monophosphate (cAMP)-dependent (large cholangiocytes) signaling.[3,5,6] In rodent liver, large cholangiocytes are the only cells that (1) express the receptor for secretin (SR), cystic fibrosis transmembrane regulator (CFTR), and Cl^-/HCO_3^- anion exchanger 2 (Cl^-/HCO_3^- AE2) and (2) secrete bicarbonate in response to secretin by activation of cAMP-dependent CFTR⇒Cl^-/HCO_3^- AE2.[1-3,5,7,8] Ca^{2+}-dependent adenylyl cyclase (AC)8 (expressed mainly by large cholangiocytes) regulates large biliary functions.[9]

Normal cholangiocytes are mitotically dormant,[5] but proliferate or are damaged in response to bile duct ligation (BDL) or acute CCl_4 administration.[5,10] The proliferative responses of cholangiocytes to these pathological maneuvers are heterogeneous and size dependent.[5,10,11] In rodents with BDL, only large cholangiocytes proliferate (thus increasing large intrahepatic bile duct mass; IBDM)[5,12] by activation of cAMP-dependent signaling.[5,12] The function of small cholangiocytes is less defined.[4,10] D-*myo*-inositol 1,4,5-trisphosphate (IP_3)/Ca^{2+}/calmodulin-dependent protein kinase (CaMK) I signaling is important in regulating small cholangiocyte function.[4] We have previously shown that concomitant with damage of large cholangiocytes,[10,11] small cholangiocytes *de novo* proliferate and acquire functional markers of large cholangiocytes to compensate for the loss of large bile ducts.[10,11] However, the mechanisms by which small cholangiocytes replenish the biliary epithelium subsequent to the damage of large ducts are unknown.

Gamma-aminobutyric acid (GABA) is the chief inhibitory neurotransmitter in the mammalian central nervous system. The liver represents the major site of synthesis and metabolism of GABA.[13] Because GABA affects cell functions by the activation of Ca^{2+}-dependent signaling and inhibition of AC activity,[14] we tested the hypothesis that GABA (1) damages large cholangiocytes and (2) induces the differentiation of small into functional large cholangiocytes by Ca^{2+}/CaMK I-dependent activation of AC8.

Materials and Methods

Materials. Reagents were purchased from Sigma-Aldrich Chemical Co. (St. Louis, MO), unless otherwise indicated. BAPTA/AM (1,2-bis-(o-aminophenoxy)-ethane-N,N,N′,N′-tetraacetic acid, tetraacetoxymethyl ester; intracellular Ca^{2+} chelator)[4] and N-(6-aminohexyl)-5-chloro-1-naphtalenesulfonamide (W7; a calmodulin antagonist that binds to calmodulin and inhibits Ca^{2+}/calmodulin-regulated enzyme activities, such as CaMK protein kinase)[4] were purchased from Calbiochem Biotechnology (San Diego, CA). Primers for real-time polymerase chain reaction (PCR) were purchased from SABiosciences (Valencia, CA). The RNeasy Mini Kit (to purify total RNA) was purchased from Qiagen Inc. (Valencia, CA). The radioimmunoassay (RIA) kits, for the measurement of cAMP (cAMP [^{125}I] Biotrak Assay System, RPA509) and IP_3 (IP_3 [^{3}H] Biotrak Assay System, TRK1000) levels, were purchased from GE Healthcare (Piscataway, NJ). Antibodies (Abs) were purchased from Santa Cruz Biotechnology (Santa Cruz, CA), unless otherwise indicated. The CFTR monoclonal Ab (immunoglobulin G1) was purchased from Thermo Fisher Scientific (Fremont, CA). The anti Cl^-/HCO_3^- AE2 Ab was obtained from Alpha Diagnostic International (San Antonio, TX).

In Vivo *and* In Vitro *Models.* Male C57/BI6N mice (20-25 g) were purchased from Charles River Laboratories (Wilmington, MA), kept in a temperature-controlled environment with 12-hour light-dark cycles and free access to water and standard chow. Studies were performed in normal mice, and mice that, immediately after BDL,[3] were treated with daily intraperitoneal (IP) injections of (1) 0.9% saline (vehicle) or (2) GABA (50 mg/kg body weight; b.w.)[15] in the absence or presence of BAPTA/AM (6 mg/kg b.w.)[16] or W7 (50 μmol/kg b.w.)[17] for 7 days. Animal surgeries and anesthesia (50 mg/kg b.w., IP) were

This work was supported partly by the Dr. Nicholas C. Hightower Centennial Chair of Gastroenterology from Scott & White, the VA Research Scholar Award, a VA Merit Award, the National Institutes of Health (grant nos.: DK062975 and DK76898; to G.A.), and by University funds (to P.O.) and PRIN 2007 and Federate Athenaeum funds from University of Rome "La Sapienza" (to E.G.).

**E.G. and G.A. share the senior authorship.*

Address reprint requests to: Gianfranco Alpini, Ph.D., Scott & White Digestive Diseases Research Center, Central Texas Veterans Health Care System, Texas A & M Health Science Center College of Medicine, Olin E. Teague Medical Center, 1901 South 1st Street, Building 205, 1R60, Temple, TX 76504. E-mail: galpini@tamu.edu; fax: 254-743-0378.

View this article online at wileyonlinelibrary.com.

DOI 10.1002/hep.26308

Potential conflict of interest: Nothing to report.

Additional Supporting Information may be found in the online version of this article.

performed in accord with protocols approved by the Scott & White and Texas A&M HSC Institutional Animal Care and Use Committee (Temple, TX). *In vitro* studies were performed in immortalized small and large cholangiocyte lines, which display morphological and functional characteristic similar to that of freshly isolated small and large cholangiocytes.[4,18]

GABA Receptor Expression. GABA receptor expression ($GABA_A$, $GABA_B$, and $GABA_C$) was evaluated by immunohistochemistry (IHC) in liver sections (4-5 μm thick). After IHC, sections were analyzed by two board-certified researchers in a blinded fashion using a BX-51 light microscope (Olympus, Tokyo, Japan) with a video camera (Spot Insight; Diagnostic Instrument, Inc., Sterling Heights, MI) and evaluated with an Image Analysis System (IAS 2000; Delta Sistemi, Rome, Italy). Expression of GABA receptors was evaluated in small and large cholangiocytes by real-time PCR and immunofluorescence (IF).[19] The primers (from SABiosciences) used are described in the Supporting Materials. A delta delta threshold cycle analysis was obtained using small cholangiocytes as control samples. Data are expressed as relative messenger RNA (mRNA) levels ± standard error of the mean (SEM) of GABA receptor/glyceraldehyde-3-phosphate dehydrogenase (GAPDH) ratio. After staining, images were visualized in a coded fashion using an Olympus IX-71 confocal microscope. For all immunoreactions, negative controls were included.

In Vivo *Studies*

Effect of GABA on Biliary Apoptosis and IBDM and the Expression of CaMK I and AC8 in Liver Sections. We measured liver morphology, lobular damage, and necrosis by hematoxylin and eosin (H&E) staining and steatosis by Oil Red staining in paraffin-embedded liver sections (4-5 μm thick, three sections evaluated per group of animals). At least 10 different portal areas were evaluated for each parameter. Liver sections were examined by two board-certified researchers in a coded fashion by a BX-51 light microscope (Olympus) equipped with a camera.

We evaluated the apoptosis of small and large cholangiocytes by quantitative terminal deoxynucleotidyl transferase biotin-dUTP nick-end labeling (TUNEL) kit (Apoptag; Chemicon International, Inc., Temecula, CA) in liver sections. TUNEL-positive cells were counted in a coded fashion in six nonoverlapping fields (magnification, ×40) for each slide; data are expressed as the percentage of TUNEL-positive cholangiocytes. The number of small and large cholangiocytes in liver sections was determined by evaluation of IBDM, which was measured as the area occupied by cytokeratin 19–positive bile duct/total area × 100. Morphometric data were obtained in six different slides for each group; for each slide, we performed, in a coded fashion, the counts in six nonoverlapping fields: n = 36.

By IHC, we evaluated, in a coded fashion, the expression of Ca^{2+}-dependent CaMK I and AC8 in liver sections from BDL mice treated with saline or GABA for 1 week. Six different slides were evaluated per group. After staining, sections were analyzed for each group using a BX-51 light microscope (Olympus).

In Vitro *Studies*

Mechanisms by Which GABA Induces the Differentiation of Small Into Large Cholangiocytes. After trypsinization, small cholangiocytes were seeded into six-well plates (500,000 cells/well) and allowed to adhere to the plate overnight. Cells were treated at 37°C with GABA (1 μM)[20,21] for 1, 3, or 7 days in the absence or presence of preincubation (2 hours) with BAPTA/AM (5 μM)[4] or W7 (10 μM).[4] Subsequently, we measured: (1) Bax (proapoptotic protein) and proliferating cellular nuclear antigen (PCNA; index of DNA replication) expression by immunoblottings in protein (10 μg) from cholangiocyte lysate (2) expression of SR, CFTR, and Cl^-/HCO_3^- AE2 by IF in cell smears, and (3) basal and secretin-stimulated cAMP levels by RIA.[3,22] For immunoblottings, band intensity was determined by scanning video densitometry using the phospho-imager, Storm 860 (GE Healthcare) and ImageQuant TL software (version 2003.02; GE Healthcare).

After treatment of small and large cholangiocytes with 0.2% bovine serum albumin (BSA; basal) or GABA (1 μM)[20,21] for 3 days, we evaluated, by scanning electron microscopy, the ultrastructural features of these cells (Supporting Materials).

For cAMP measurements, after GABA treatment (1 μM for 3 days), small cholangiocytes (1×10^5) were stimulated at room temperature for 5 min with: (i) 0.2% BSA or secretin (100 nM) in the absence/presence of 5-min preincubation with BAPTA/AM (5 μM) or W7 (10 μM)

Role of CaMK I in GABA-Induced Differentiation of Small Into Large Cholangiocytes. We have developed a stable-transfected small mouse cholangiocyte line characterized by decreased expression of the CaMK I gene.[4] We evaluated, by IF, whether small control vector- or CaMK I short hairpin RNA (shRNA)-transfected cholangiocytes express GABA receptors. Then, we performed studies to demonstrate that (1) GABA increases IP_3 levels, mRNA, and/or protein expression for

CaMK I and AC8 in small cholangiocytes[4] and (2) silencing of CaMK I in small cholangiocytes prevents GABA-induced differentiation of small into large cholangiocytes and AC8 activation. The primers (from SABiosciences) used are described in the Supporting Materials.

Knockdown (~70%)[4] of the CaMK I gene in small cholangiocytes was established by a SureSilencing shRNA (SABiosciences) plasmid for mouse CaMK I, containing the gene for neomycin (geneticin) resistance for selection of transfected cells.[4] Control or CaMK I shRNA-transfected small cholangiocytes were incubated at 37°C with GABA (1 μM) for 3 days before evaluating (1) expression of GABA receptors by IF, (2) PCNA protein expression by immunoblottings, (3) expression of SR, CFTR, and Cl^-/HCO_3^- AE2 by IF in a coded fashion, and (4) basal and secretin-stimulated cAMP levels by RIA.[3,22]

Role of AC8 on GABA-Induced Differentiation of Small Into Large Cholangiocytes. Because AC8 regulates the function of large cholangiocytes,[9] we proposed to demonstrated that IP_3/Ca^{2+}/CaMK I-dependent, GABA-induced differentiation of small into large cholangiocytes are dependent on the presence or activation of AC8. Thus, we studied: (1) biliary expression of AC8 (by IHC) in liver sections and small cholangiocytes from BDL mice treated with saline or GABA for 1 week and (2) message expression of AC8 by real-time PCR[4] in control vector- or CaMK I shRNA-transfected small cholangiocytes treated with 0.2% BSA or GABA (1 μM) for 3 days. We studied the effect of *in vitro* GABA treatment (1 μM, 3 days) in the absence or presence of preincubation (2 hours) with the AC8 inhibitor, 2′-deoxyadenosine 3′-monophosphate (10 mM),[23] on the differentiation of small into large cholangiocytes by measuring the semiquantitative expression of SR, CFTR, and Cl^-/HCO_3^- AE2 by IF. The primers used are shown in the Supporting Materials.

Statistical Analysis. Data are expressed as mean ± SEM. Differences between groups were analyzed by the Student unpaired *t* test when two groups were analyzed and by analysis of variance when more than two groups were analyzed, followed by an appropriate post-hoc test. Mann-Whitney's U test was used to determine ultrastructural differences between cells treated with BSA or GABA. For SEM, statistical analyses were performed using SPSS statistical software (SPSS, Inc., Chicago, IL).

Results

Evaluation of GABA Receptor Expression. Both small (yellow arrows) and large (red arrows) bile ducts from normal (not shown) and BDL (treated with vehicle or GABA) mice express $GABA_A$, $GABA_B$, and $GABA_C$ receptors (Fig. 1A). By real-time PCR and IF (Fig. 1B,C), small and large cholangiocyte lines express the three GABA receptor subtypes.

In Vivo *Studies*

Effect of GABA on Biliary Proliferation and Apoptosis. H&E and Oil Red staining of liver sections show that there were no significant differences in degree of lobular damage, necrosis, and steatosis among the several groups (not shown).

Administration of GABA to BDL mice increased the percentage of apoptosis of large cholangiocytes, compared to vehicle-treated BDL mice (Fig. 2A). Small bile ducts were resistant to GABA-induced apoptosis (Fig. 2A). Consistent with the concept that IP_3/Ca^{2+}/CaMK I signaling regulates the function of small cholangiocytes,[4] blockage of this pathway by BAPTA/AM or W7 (administered together with GABA) increased apoptosis in small bile ducts, compared to BDL mice treated with saline or GABA alone (Fig. 2A).

IBDM was higher in large, compared to small, cholangiocytes (Fig. 2B). There was decreased large IBDM (Fig. 2B) and *de novo* proliferation of small cholangiocytes with increased small IBDM (Fig. 2B). GABA stimulation of small IBDM was partly blocked by BAPTA/AM and W7 (Fig. 2).

In Vitro *Studies*

Effect of GABA on Apoptosis and Proliferation of Small Cholangiocytes and the Functional Switch of Small Into Large Cholangiocytes. There were no changes in Bax protein expression in small cholangiocytes treated with GABA, compared to basal (Fig. 3A). GABA increased PCNA protein expression in small cholangiocytes, compared to basal (Fig. 3B), an increase that was blocked by preincubation with BAPTA/AM and W7 (Fig. 3B). There were no differences in expression of Bax and PCNA in small cholangiocytes treated with 0.2% BSA for time zero, 1, 3, or 7 days (not shown). Our basal values (Fig. 3A,B) correspond to 3 days of BSA treatment.

The study performed by scanning electron microscopy aimed to analyze the ultrastructural features of the cell surface, shows that large cholangiocytes (basal treatment) show a surface with a high density of microvilli and the presence of a primary cilium for each cell (the cilium characterizes a large or mature cholangiocyte)[24] (Fig. 3C). Subsequent to GABA treatment, large cholangiocytes show a not-well-preserved morphology, a decrease in microvilli density, and an absence of primary cilia (Fig. 3C). Small cholangiocytes

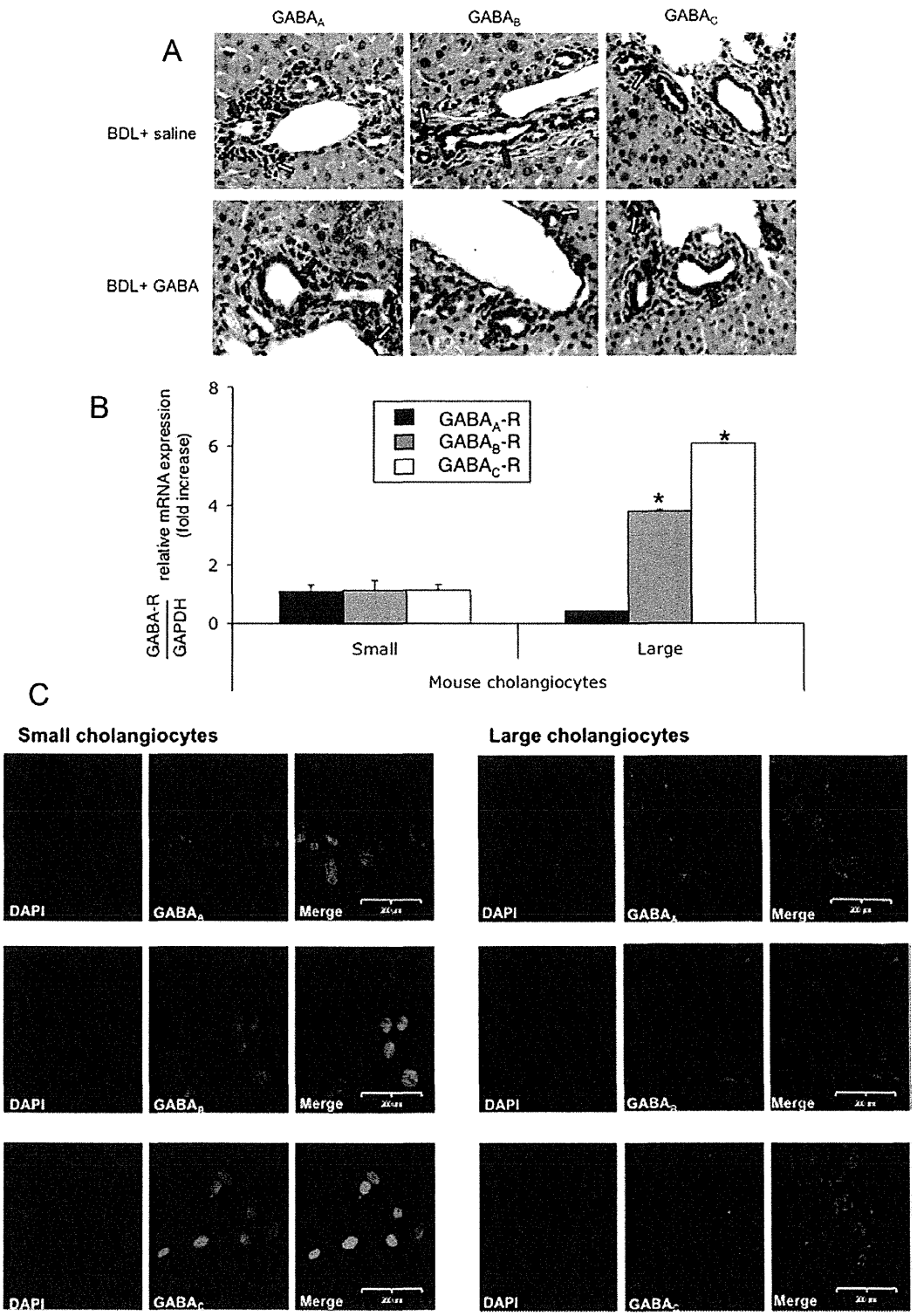

Fig. 1. (A) Both small (yellow arrows) and large (red arrows) intrahepatic bile ducts from BDL mice (treated with vehicle or GABA) express $GABA_A$, $GABA_B$, and $GABA_C$ receptor subtypes. Original magnification: ×40. (B and C) By PCR and IF, small and large cholangiocyte lines express the three GABA receptor subtypes. Data are mean ± SEM of three PCR reactions. *$P < 0.05$ versus expression of GABA receptors in small cholangiocytes. (C) Specific immunoreactivity of representative fields is shown in green, and nuclei were stained with 4′,6-diamidino-2-phenylindole (DAPI; blue). Bar = 200 μm.

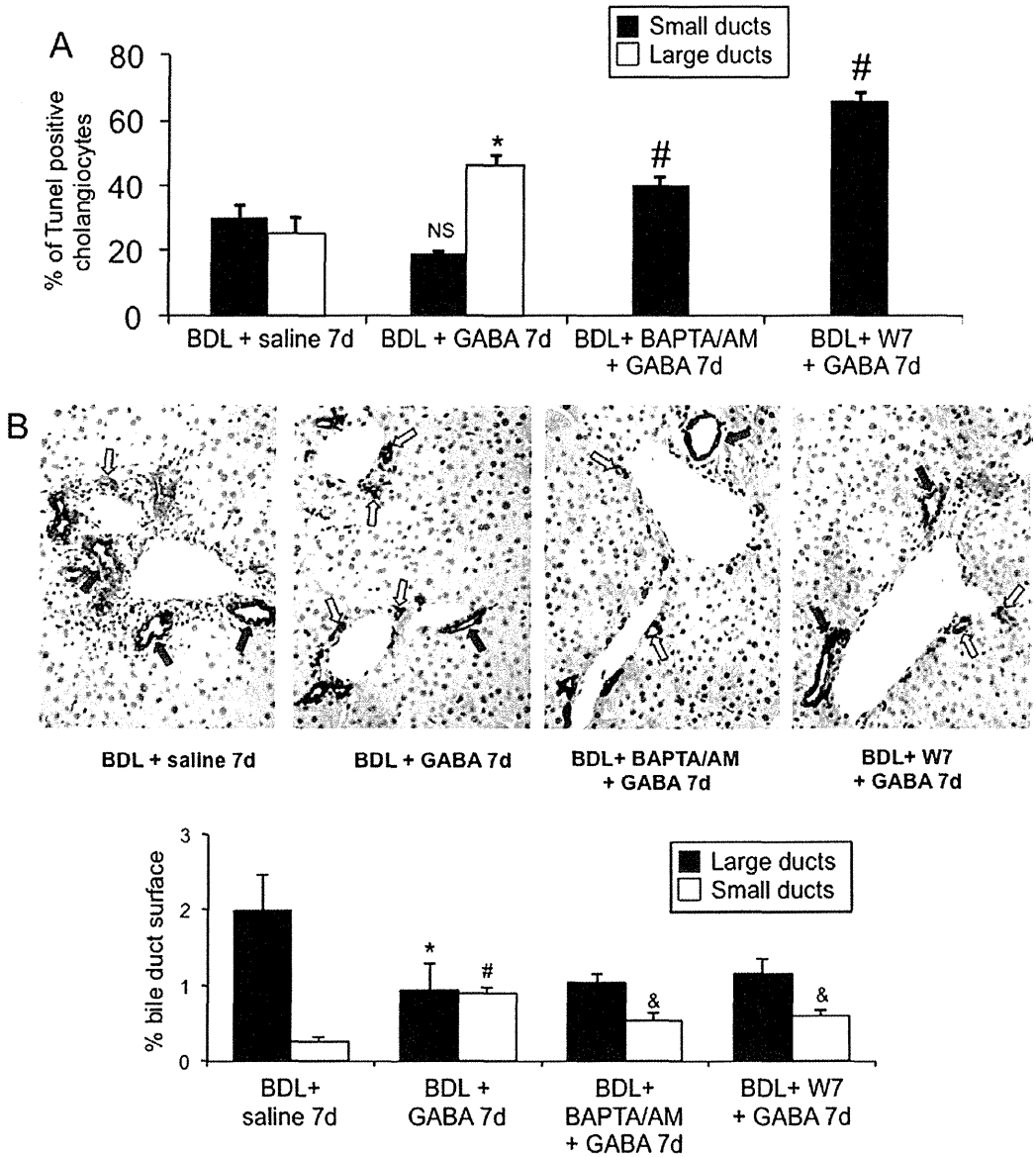

Fig. 2. (A and B) Evaluation of apoptosis and IBDM of small and large cholangiocytes in liver sections from BDL mice treated with vehicle or GABA for 1 week. (A) Administration of GABA to BDL mice increased the percentage of apoptosis of large cholangiocytes, compared to controls. *$P < 0.05$ versus apoptosis of large cholangiocytes from BDL mice treated with vehicle. #$P < 0.05$ versus apoptosis of small cholangiocytes from BDL mice treated with saline or GABA alone. (B) After administration of GABA to BDL mice, there was decreased large IBDM and the *de novo* proliferation of small cholangiocytes partly blocked by BAPTA/AM and W7. Original Magnification: ×20. *$P < 0.05$ IBDM of large cholangiocytes from BDL mice treated with NaCl versus BDL+GABA; #$P < 0.05$ IBDM of small cholangiocytes from BDL versus BDL+GABA; &$P < 0.05$ IBDM of small cholangiocytes from BDL+GABA versus BDL+GABA+BAPTA/AM and BDL+GABA+W7. Yellow arrows: small ducts; red arrows: large ducts.

show a cell size slightly reduced, compared with large cholangiocytes, few microvilli, and the absence of primary cilia (Fig. 3C). Small cholangiocytes treated *in vitro* with GABA for 3 days show an increase in cellular size and a higher density of microvilli, compared to basal (Fig. 3C).

Large (not shown), but not small (Fig. 4A), cholangiocytes express SR, CFTR, and Cl^-/HCO_3^- AE2. Subsequent to *in vitro* GABA treatment, small cholangiocytes *de novo* express SR, CFTR, and Cl^-/HCO_3^- AE2 (Fig. 4A). As expected,[3] secretin increased cAMP levels of large cholangiocytes (not shown). When small cholangiocytes were treated with GABA for 3 days *in vitro*, there were increased basal cAMP levels and *de novo* responsiveness to secretin with increased cAMP levels (Fig. 4B). GABA-induced increases in secretin-

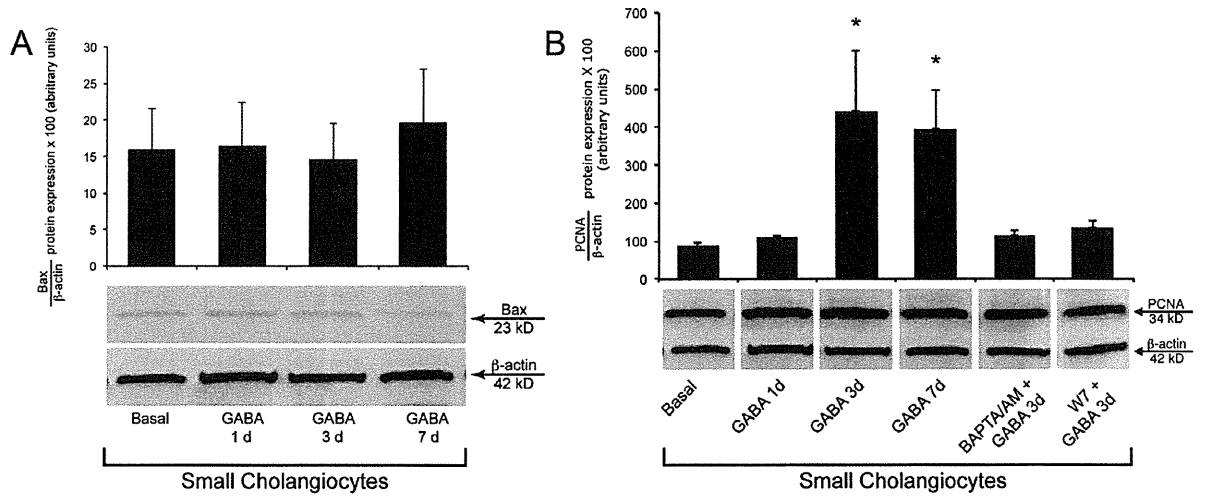

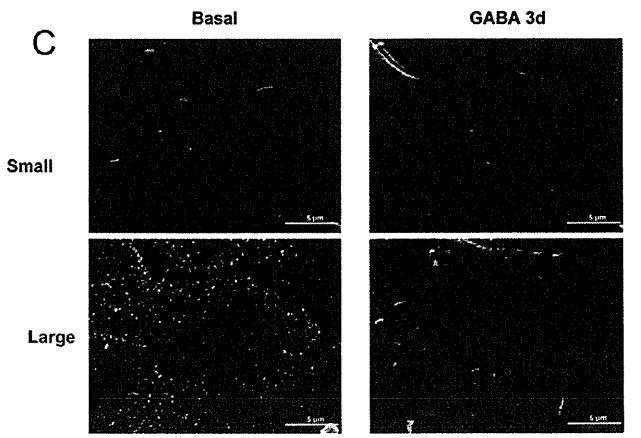

	Cell size (μm ± SEM)	Microvilli density (n/surface ± SEM)
Small basal	10.3 ± 0.6	155.6 ± 7.8
Small + GABA 3d	11.6 ± 0.4	195.2 ± 6.7^
Large basal	13.2 ± 0.1	357.7 ± 18.2
Large + GABA 3d	12.1 ± 0.2&	213.2 ± 15.0*

Fig. 3. Evaluation of (A) apoptosis and (B) proliferation of small and large cholangiocytes treated for with BSA or GABA (1 μM) in the absence or presence of selected inhibitors. (A) Data are mean ± SEM of eight western blots. (B) Data are mean ± SEM of 11 immunoblottings. *$P < 0.05$ versus the corresponding basal value. (C) Scanning electron microscopy of small and large cholangiocytes treated with BSA or GABA (1 μM) for 3 days. Small cholangiocytes show a cell size slightly reduced, compared to large cholangiocytes, fewer microvilli, and the absence of primary cilia. Small cholangiocytes treated *in vitro* with GABA for 3 days show a weak increase in cellular size, compared to small cholangiocytes, and a higher density of microvilli. Data are indicated as mean ± SEM. $P < 0.05$ was considered statistically significant. Cell size: small plus BSA versus small plus GABA ($P = 0.18$; not significant); &large plus BSA versus large plus GABA ($P < 0.05$). Microvilli density: ^small plus BSA versus small plus GABA ($P < 0.05$); *large plus BSA versus large plus GABA ($P < 0.05$).

stimulated cAMP levels were blocked by BAPTA/AM and W7 (Fig. 4B).

Role of CaMK I in GABA-Induced Differentiation of Small Into Large Cholangiocytes. Both vector- (not shown) and CaMK I-transfected small cholangiocytes express all three GABA receptors (not shown). *In vivo* administration of GABA to BDL mice increased the expression of CaMK I protein in small ducts (Fig. 5A). GABA (after 3 days of *in vitro* treatment) increased IP_3 levels and CaMK I expression of small cholangiocytes (Fig. 5B). Knockdown of CaMK I in small cholangiocytes blocked (1) stimulatory effects of GABA on PCNA protein expression (Fig. 6A), (2) GABA-induced *de novo* acquisition of SR, CFTR, and

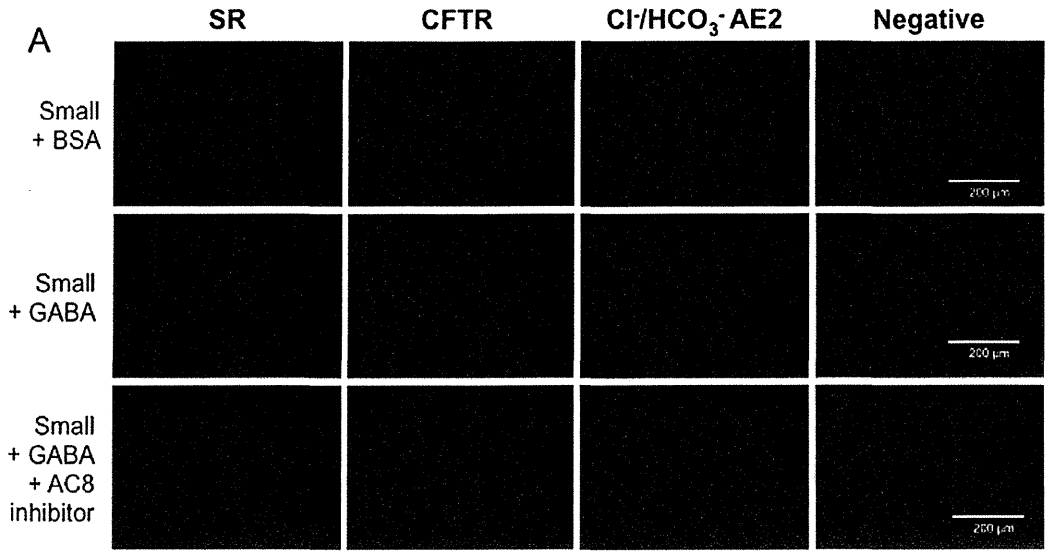

	SR	CFTR	Cl-/HCO3- AE2
Small + BSA	-	-	-
Small + GABA	+	+	+
Small + GABA + AC8 inhibitor	+/-	+/-	+/-

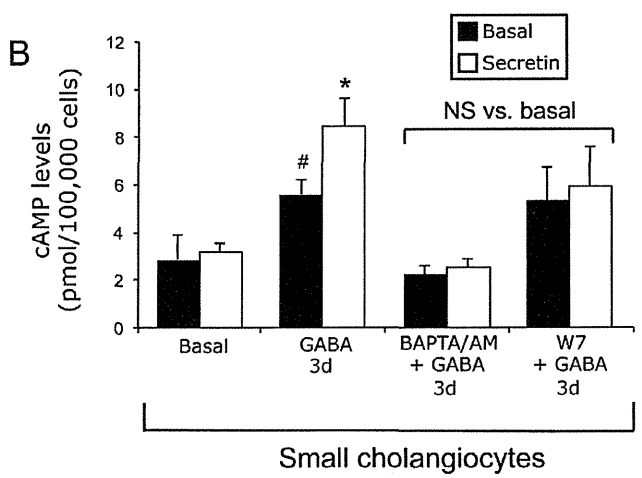

Fig. 4. (A) Representative IF for SR, CFTR, and Cl^-/HCO_3^- AE2 exchanger in small mouse cholangiocytes treated with BSA, GABA (1 μM), or AC8 inhibitor plus GABA (1 μM) for 3 days. After *in vitro* GABA treatment, small cholangiocytes *de novo* acquire these proteins. GABA-induced *de novo* expression of SR, CFTR, and Cl^-/HCO_3^- AE2 was reduced by the AC8 inhibitor. Bar = 200 μm. (B) Measurement of basal and secretin-stimulated cAMP levels in small cholangiocytes treated for 3 days with 0.2% BSA (or GABA) (1 μM in the absence or presence of selected inhibitors) for 3 days. In small cholangiocytes treated with GABA, there were increased basal cAMP levels. When small cholangiocytes were treated with GABA, these cells *de novo* respond to secretin with increased cAMP levels. In small cholangiocytes, *de novo* secretin-stimulated cAMP levels were blocked by BAPTA/AM and W7. Data are mean ± SEM of 11 experiments. #$P < 0.05$ versus the corresponding basal value of cholangiocytes treated with BSA.

Cl^-/HCO_3^- AE2 (Fig. 6B), and (3) *de novo* secretin-stimulated cAMP levels (Fig. 6C).

Role of AC8 in CaMK I-Dependent GABA Differentiation of Small Into Large Cholangiocytes. Subsequent to *in vivo* administration of GABA to BDL mice, there was enhanced AC8 protein expression in small ducts, expression that was blocked by pretreatment with BAPTA/AM and W7 (Fig. 7A,B). Subsequent to *in vitro* treatment with GABA (3 days, 1 μM), there was increased AC8 mRNA expression in vector-transfected small cholangiocytes (Fig. 7C). GABA did not increase the expression of AC8 in small

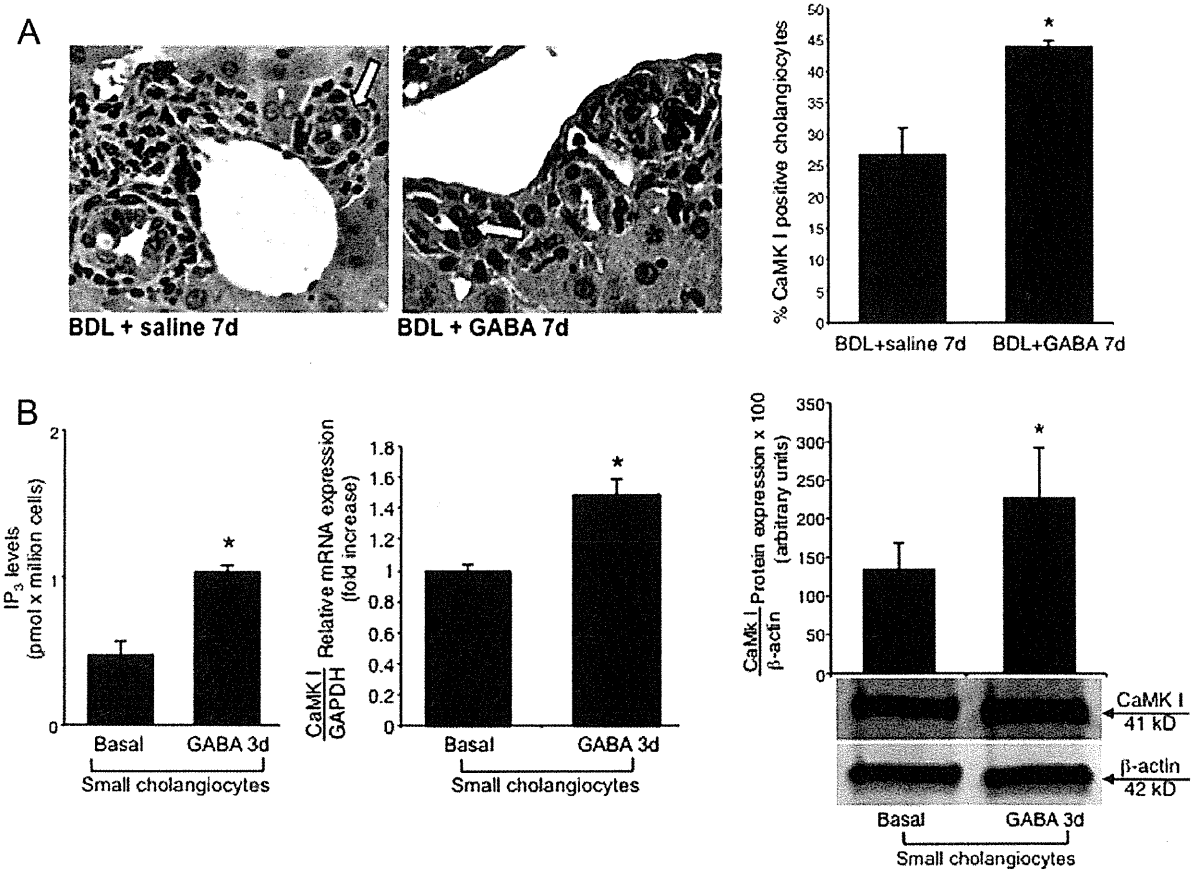

Fig. 5. (A) Measurement of CaMK I protein expression in liver sections from BDL mice treated *in vivo* with saline or GABA for 1 week. Administration of GABA to BDL mice increased the expression of CaMK I in small bile ducts. Original Magnification: x40. *$P < 0.05$ versus the corresponding basal value of BDL mice treated with saline. (B) Evaluation of IP_3 levels (18 evaluations) and CaMK I expression (by PCR and immunoblots; n = 4) in small cholangiocytes treated *in vitro* with GABA (3 days at 1 μM). *$P < 0.05$ versus the corresponding basal value.

cholangiocytes transfected with CaMK I shRNA (Fig. 7C). GABA-induced *de novo* (1) activation of PCNA expression (see Fig. 3B), and (2) expression of SR, CFTR, and Cl^-/HCO_3^- AE2 (Fig. 4A) of small cholangiocytes was blocked by the AC8 inhibitor.

Discussion

Our findings relate to the functional switch of small into large cholangiocytes after prolonged *in vivo* and *in vitro*: GABA treatment. We have shown that small and large cholangiocytes express the three GABA receptor subtypes. *In vivo* administration of GABA: (1) induces apoptosis of large, but not small, cholangiocytes and (2) decreased large IBDM, but increased *de novo* small IBDM, in BDL mice. GABA stimulation of small IBDM was partly blocked by BAPTA/AM and W7. The *in vivo* data support our recent studies[11] in BDL rats, where GABA induced damage of large ducts and the *de novo* proliferation of small cholangiocytes. However, our recent *in vivo* studies in rats[11] *did not* (1) demonstrate the direct effects of GABA on cholangiocyte functions, effects that could be nonspecific and mediated by the release of unidentified growth factors, and (2) address the mechanisms by which GABA induces *in vitro* the differentiation of small into large cholangiocytes. Thus, we proposed to develop an *in vitro* model in which GABA interacts with receptors on cholangiocytes and induces differentiation of small into large functional cholangiocytes by activation of IP_3/Ca^{2+}/CaMK I-dependent AC8 signaling. The differentiation of small into large cholangiocytes (evidenced by the *de novo* acquisition of ultrastructural and functional phenotypes of large cholangiocytes) was associated with increased (1) IP_3 levels and CaMK I phosphorylation and (2) expression of AC8 in small cholangiocytes. In small cholangiocytes, knockdown of the CaMK I gene prevented (1) GABA-induced differentiation into large cholangiocytes and (2) GABA-induced increase of AC8. The study has important clinical implications, because, in pathological

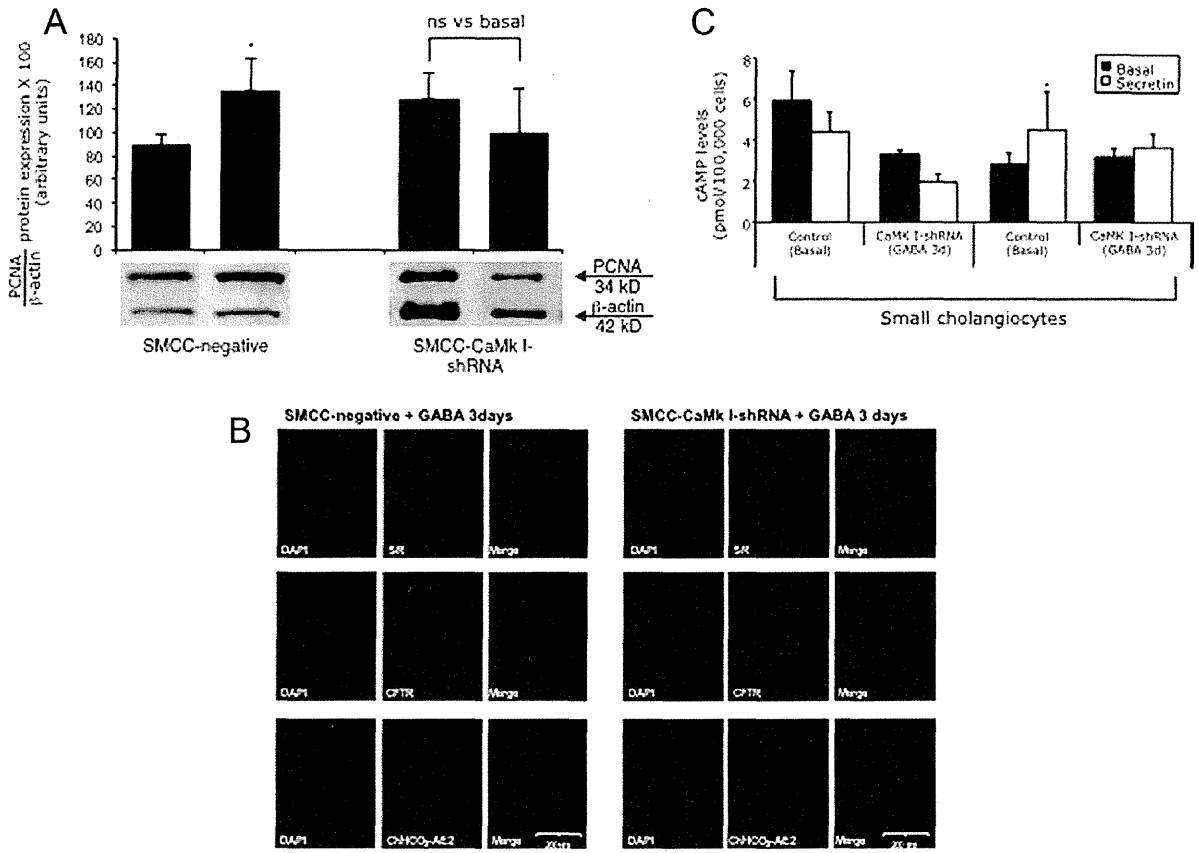

Fig. 6. Effect of CaMK I silencing on GABA-induced (A) PCNA protein expression, (B) acquisition of SR, CFTR, and Cl^-/HCO_3^- AE2, and (C) *de novo* secretin-stimulated cAMP levels of small cholangiocytes. Knockdown of CaMK I in small cholangiocytes blocked the stimulatory effects of GABA on (A) PCNA protein expression, GABA-induced *de novo* acquisition of SR, CFTR, and Cl^-/HCO_3^- AE2 (B), and *de novo* secretin-stimulated cAMP levels (C) in small cholangiocytes. $^*P < 0.05$ versus the corresponding basal value of small cholangiocytes transfected with empty vector. Data are mean ± SEM of eight blots. For cAMP measurements, data are mean ± SEM of 10 evaluations.

conditions associated with damage/loss of large ducts, the proliferation of small cholangiocytes and the differentiation of these cells into large cholangiocytes may be key in the replenishment of the biliary epithelium.

We first performed *in vivo* studies in BDL mice to demonstrate the decrease of large IBDM and *de novo* proliferation of small ducts after GABA *in vivo* administration. Small and large cholangiocytes differentially respond to liver injury with changes in apoptotic, proliferative, and secretory activities.[5,10,25] After BDL, only large cholangiocytes proliferate, leading to increased IBDM and secretin-stimulated choleresis by activation of cAMP signaling.[5,10] After damage of large ducts by CCl_4, small cholangiocytes (resistant to CCl_4-induced apoptosis) *de novo* proliferate and acquire large cholangiocyte phenotypes to compensate for the loss of large duct functions.[10] The mechanisms by which small cholangiocytes acquire phenotypes of large cholangiocytes are unknown. The differential apoptotic and proliferative responses to GABA *in vitro* treatment does not depend on the different expression of GABA receptors, because both small and large cholangiocytes express the three GABA receptors that likely mediate these effects. Indeed, our recent study[20] in human cholangiocarcinoma cells has shown that blocking of $GABA_A$, $GABA_B$, and $GABA_C$ receptors prevents GABA inhibition of cholangiocarcinoma proliferation.

The reason why GABA damages only large ducts may also be the result of sensitization from obstructive cholestasis and subsequent biliary/seric accumulation[26] as well as dysregulation of GABA metabolism during liver damage.[27] The higher resistance of small cholangiocytes to GABA may also depend on their more undifferentiated nature, whereas large (more differentiated) cholangiocytes are more susceptible to injury.[11] Indeed, the presence of a larger nucleus and a smaller cytoplasm in small cholangiocytes suggests the undifferentiated nature of these cells.[28] Large cholangiocytes (displaying a larger cytoplasm) are perhaps more

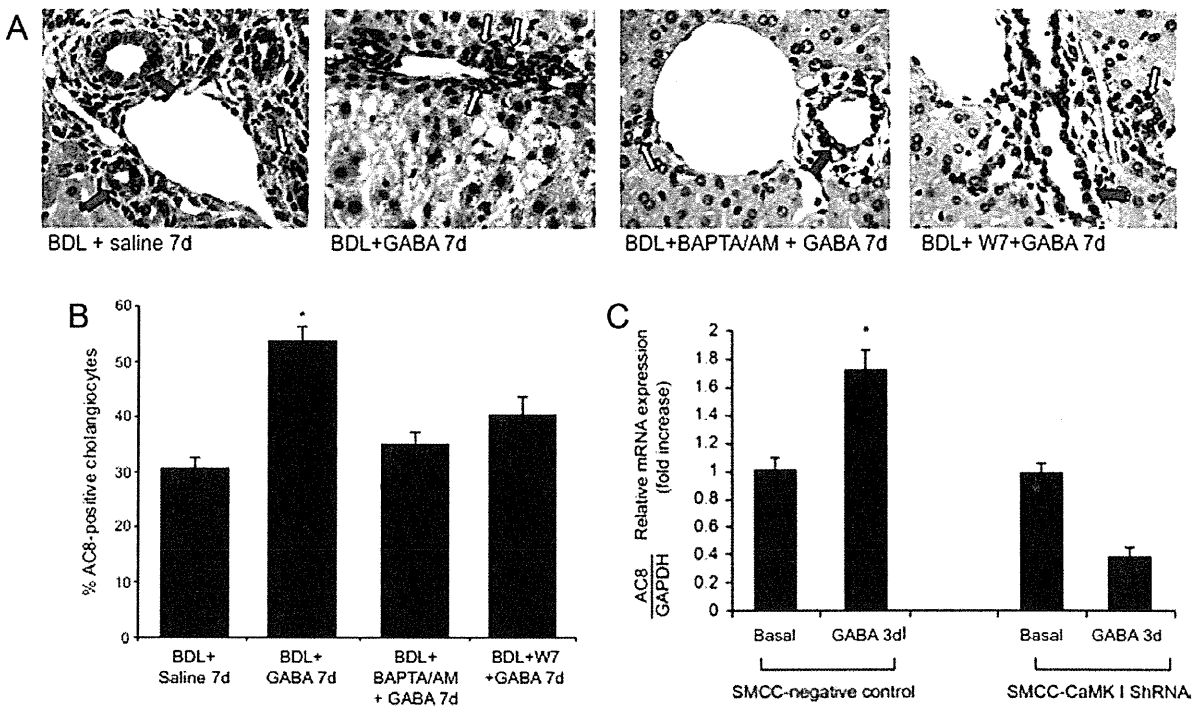

Fig. 7. (A) Measurement of AC8 expression by IHC in liver sections from BDL mice treated with saline or GABA in the absence or presence of BAPTA/AM or W7 for 1 week. Original Magnification: ×40. Yellow arrows: small ducts; red arrows: large ducts. (B) Measurement of AC8 expression (by real-time PCR) in mock- or CaMK I-transfected small cholangiocytes treated *in vitro* with BSA or GABA. GABA-induced increase in AC8 in small cholangiocytes was blocked by CaMK I knockdown. Data are mean ± SEM of three experiments.

differentiated cells and more susceptible to damage.[28] The higher expression of the antiapoptotic protein, B-cell lymphoma 2, by small ducts in normal and cirrhotic human liver may also explain the higher resistance of small cholangiocytes to injury.[29] The higher expression of Ca^{2+}-dependent signaling may contribute to the higher resistance of the small cholangiocyte compartment to injury, as suggested in other cell systems.[30]

We propose several speculations to explain why small cholangiocytes differentiate *in vivo* into large cholangiocytes when the latter cells are damaged. During damage of large ducts, there must be a compensatory mechanism in the biliary epithelium (represented by small bile duct compartment) that is activated (acquiring traits of large cholangiocytes)[10,31] to maintain the homeostasis of the biliary tree. Also, the differentiation of small, undifferentiated cholangiocytes into large (more senescent) cholangiocytes may be a natural process of senescence accelerated by GABA. Our findings parallel the pathophysiology of the intestine, where there is intestinal epithelial cell maturation along the crypt-villus axis,[32] an event that is regulated by changes in the intestine microenvironment and neuroendocrine interactions.[33] Similar to previous studies,[34] we propose that changes in the biliary microenvironment may partly explain the effect of GABA on small and large cholangiocytes.

Another interesting aspect to consider regards the possible role of GABA receptor antagonists in experimental models and human pathologies. When the liver of BDL rats is deprived of cholinergic (by vagotomy) or adrenergic (by 6-hydroxydopamine) innervation, large cholangiocytes lose their response to cholestasis and undergo apoptosis, reducing cAMP levels and the choleretic response to secretin.[35,36] The damage and loss of proliferative and secretory functions of cholangiocytes, by vagotomy and 6-OHDA, is prevented by the administration of forskolin, and β1-/β2-adrenergic receptor agonists.[35,36] Because GABA concomitantly damages large cholangiocytes and induces ductular reaction, we speculate that the administration of GABA receptor antagonists may prevent the damage of large cholangiocytes (sustaining large biliary proliferation and secretion) in the denervated liver. This may be important for the homeostasis of the transplanted (denervated) liver, where ischemic or infectious insults against intrahepatic bile ducts may not be adequately counteracted during the immediate post-transplant period.

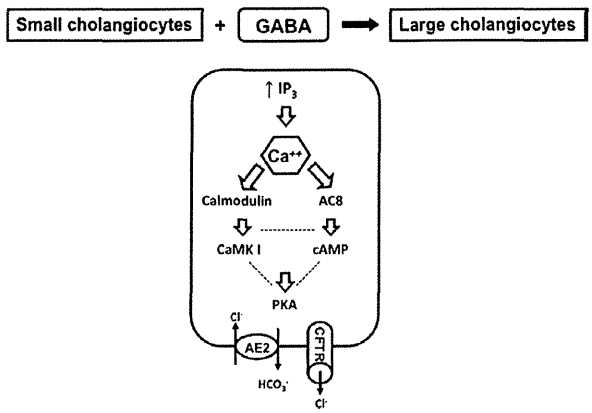

Fig. 8. Cartoon describing the differentiation of Ca^{2+}-dependent cholangiocytes into cells that (in addition to maintaining their Ca^{2+}-dependent signaling) express markers of large cholangiocytes by Ca^{2+}/CaMK I-dependent activation of AC8. In this model, after chronic *in vitro* treatment, small cholangiocytes acquire markers of large cholangiocytes and, *de novo*, respond to secretin with changes in secretory activity.

The finding that the activation of IP_3/Ca^{2+}-dependent signaling regulates the differentiation of small into large cholangiocytes supports the concept that cross-talk between IP_3/Ca^{2+} and cAMP is important in the regulation of biliary homeostasis. For example, alpha-1 adrenergic receptor agonists stimulate secretin-stimulated choleresis of BDL rats by Ca^{2+}- and protein kinase C (PKC)α/βII-dependent activation of cAMP signaling.[37] Gastrin inhibits cAMP-dependent secretion and hyperplasia in BDL rats by activation of Ca^{2+}-dependent PKCα.[38] In support of our findings, activation of the Ca^{2+}/calcineurin/NFAT2 pathway controls smooth muscle cell differentiation.[39] Ca^{2+} ions regulate the differentiation and proliferation of human bone-marrow–derived mesenchymal stem cells.[40] In this study, we have identified two signaling molecules (CaMK I and AC8) playing major roles in the differentiation of Ca^{2+}-dependent small into large cholangiocytes. Previous studies in other cells support the concept that CaMK I regulates the expression of AC8.[41] In fact, when secretion was induced by forskolin, a general stimulator of AC isoforms, except for AC9 and sAC, administration of calmodulin inhibitors and AC8 small interfering RNA did not cause a significant inhibitory effect.[9] AC8 is the only known calmodulin-activated AC in cholangiocytes, whereas AC9 activity is inhibited by calmodulin.

We have developed a novel *in vitro* model where, after *in vitro* treatment, small cholangiocytes acquire (by Ca^{2+}/CaMK I-dependent activation of AC8) markers of large cholangiocytes and, *de novo*, respond to secretin with changes in secretory activity (Fig. 8). Activation of the small cholangiocyte "niche" and the subsequent ductular reaction may be an important compensatory mechanism to replenish the biliary epithelium in pathologies of large bile ducts.

Acknowledgment: The authors thank Bryan Moss, Medical Illustration Scott & White, for the preparation of the figures.

References

1. Alpini G, Glaser S, Robertson W, Rodgers RE, Phinizy JL, Lasater J, LeSage G. Large but not small intrahepatic bile ducts are involved in secretin-regulated ductal bile secretion. Am J Physiol Gastrointest Liver Physiol 1997;272:G1064-G1074.
2. Alpini G, Ulrich C, Roberts S, Phillips JO, Ueno Y, Podila PV, et al. Molecular and functional heterogeneity of cholangiocytes from rat liver after bile duct ligation. Am J Physiol Gastrointest Liver Physiol 1997; 272:G289-G297.
3. Glaser S, Gaudio E, Rao A, Pierce LM, Onori P, Franchitto A, et al. Morphological and functional heterogeneity of the mouse intrahepatic biliary epithelium. Lab Invest 2009;89:456-469.
4. Francis H, Glaser S, DeMorrow S, Gaudio E, Ueno Y, Venter J, et al. Small mouse cholangiocytes proliferate in response to H1 histamine receptor stimulation by activation of the IP_3/CaMK I/CREB pathway. Am J Physiol Cell Physiol 2008;295:C499-C513.
5. Alpini G, Glaser S, Ueno Y, Pham L, Podila PV, Caligiuri A, et al. Heterogeneity of the proliferative capacity of rat cholangiocytes after bile duct ligation. Am J Physiol Gastrointest Liver Physiol 1998;274:G767-G775.
6. Kanno N, LeSage G, Glaser S, Alvaro D, Alpini G. Functional heterogeneity of the intrahepatic biliary epithelium. HEPATOLOGY 2000;31: 555-561.
7. Alpini G, Roberts S, Kuntz SM, Ueno Y, Gubba S, Podila PV, et al. Morphological, molecular, and functional heterogeneity of cholangiocytes from normal rat liver. Gastroenterology 1996;110:1636-1643.
8. Alpini G, Lenzi R, Sarkozi L, Tavoloni N. Biliary physiology in rats with bile ductular cell hyperplasia. Evidence for a secretory function of proliferated bile ductules. J Clin Invest 1988;81:569-578.
9. Strazzabosco M, Fiorotto R, Melero S, Glaser S, Francis H, Spirli C, Alpini G. Differentially expressed adenylyl cyclase isoforms mediate secretory functions in cholangiocyte subpopulation. HEPATOLOGY 2009;50:244-252.
10. LeSage G, Glaser S, Marucci L, Benedetti A, Phinizy JL, Rodgers R, et al. Acute carbon tetrachloride feeding induces damage of large but not small cholangiocytes from BDL rat liver. Am J Physiol Gastrointest Liver Physiol 1999;276:G1289-G1301.
11. Mancinelli R, Franchitto A, Gaudio E, Onori P, Glaser S, Francis H, et al. After damage of large bile ducts by gamma-aminobutyric acid, small ducts replenish the biliary tree by amplification of calcium-dependent signaling and de novo acquisition of large cholangiocyte phenotypes. Am J Pathol 2010;176:1790-1800.
12. Francis H, LeSage G, DeMorrow S, Alvaro D, Ueno Y, Venter J, et al. The alpha2-adrenergic receptor agonist UK 14,304 inhibits secretin-stimulated ductal secretion by downregulation of the cAMP system in bile duct-ligated rats. Am J Physiol Cell Physiol 2007;293:C1252-C1262.
13. Erlitzki R, Gong Y, Zhang M, Minuk G. Identification of gamma-aminobutyric acid receptor subunit types in human and rat liver. Am J Physiol Gastrointest Liver Physiol 2000;279:G733-G739.
14. Martin C, Jacobi JS, Nava G, Jeziorski MC, Clapp C, Martinez de la Escalera G. GABA inhibition of cyclic AMP production in immortalized GnRH neurons is mediated by calcineurin-dependent dephosphorylation of adenylyl cyclase 9. Neuroendocrinology 2007;85:257-266.
15. Zhang M, Gong YW, Minuk GY. The effects of ethanol and gamma aminobutyric acid alone and in combination on hepatic regenerative activity in the rat. J Hepatol 1998;29:638-641.